High-temperature spin dynamics in the one-dimensional Heisenberg system $(CH_3)_4NMnCl_3$ (TMMC): Spin diffusion, intra- and interchain cutoff effects

J-P. Boucher, M. Ahmed Bakheit,* and M. Nechtschein

Département de Recherche Fondamentale, Section de Résonance Magnétique, Centre d'Etudes Nucléaires de Grenoble, B.P. 85, Centre de tri, 38041 Grenoble Cedex, France

M. Villa, G. Bonera, and F. Borsa

Istituto di Fisica Generale "A. Volta," Università di Pavia, and Gruppo Nazionale di Struttura della Materia del Consiglio Nazionale delle Ricerche, Pavia, Italy

(Received 29 May 1975)

High-temperature spin dynamics in the one-dimensional (1d) Heisenberg system $(CH_3)_4NMnCl_3$ (TMMC), is investigated through EPR and proton spin relaxation-time measurements. When the magnetic field $\vec{H}$ is parallel to the chain axis $\vec{c}$ the field dependence of both the relaxation rate T_1^{-1} and the relaxation rate in the rotating frame $T_{1\rho}^{-1}$ fits well an expression of the form $PH^{-1/2}+Q$. The $H^{-1/2}$ term in this expression proves that the spectral density $f^+(\omega)\propto\langle S_i^+(t)S_i^-(0)\rangle$ behaves according to a 1d diffusive law $f^+(\omega)\propto(D\omega)^{-1/2}$ where D represents the diffusion coefficient of the electronic two-spin correlation functions. When $\vec{H}\perp\vec{c}$ the T_1^{-1} and $T_{1\rho}^{-1}$ data show a quite different behavior, being almost constant or decreasing slightly at low field. Such a behavior is interpreted in terms of cutoff effects which limit the $1d$ diffusive behavior of the spectral density $f^z(\omega)\propto\langle S_i^z(t)S_j^z(0)\rangle$. A cutoff frequency ω_c^z is defined as the frequency at which the $\omega^{-1/2}$ divergence in $f^z(\omega)$ is truncated. The value, the field dependence, and the orientation dependence of ω_c^z show that the cutoff mechanisms are originated from electronic intrachain dipolar and interchain Heisenberg interactions. A theory is presented taking into account both intra- and interchain interactions. Self-consistent expressions are given for evaluating the cutoff frequencies. When $\vec{H}\perp\vec{c}$, the field dependence of the cutoff frequency fits the diffusive law: $(\omega_c^z)_\perp=AH^{-1/2}+B$. This is explained by considering that the cutoff mechanism is dominated by the intrachain dipolar interactions $\mathfrak{D}$. It is formally shown that the $H^{-1/2}$ dependence of $(\omega_c^z)_\perp$ and the non-Lorentzian shape of the EPR line have the same origin: They both express the diffusive behavior of the total spin torque (TST) correlation function $\propto\langle[S^+,\mathfrak{D}](t)[\mathfrak{D},S^-]\rangle$. Quantitative determinations for the diffusion coefficients of the two-spin and TST correlation functions yield $D=(2.2\pm0.2)4J[S(S+1)/3]^{1/2}$ and $D_{TST}=(4.8\pm1.2)4J[S(S+1)/3]^{1/2}$. When $\vec{H}\parallel\vec{c}$ the cutoff frequency is almost field independent. This result agrees with a cutoff mechanism originated from interchain Heisenberg interactions. The interchain coupling is evaluated to be $J/k\simeq1.3\times10^{-2}$ K.

I. INTRODUCTION

Early theoretical studies of magnetic linear chains were mainly motivated by the much greater simplicity of calculation as compared with corresponding three-dimensional systems.[1] Exact calculations in one dimension (1d) are of particular importance to obtain the general behavior of the magnetic systems and to learn about approximation procedures to be used in higher dimensions. The recent discovery of a large number of magnetic systems which behave approximately like 1d systems has given the calculations in linear magnetic chains a real and concrete interest since the predictions of the theory can now be compared directly to experimental results.[2]

The study of spin dynamics is particularly challenging since no exact theoretical solution can usually be obtained over the whole time interval and for all wavelengths even for 1d models. In the long-wavelength and long-time limit the temporal evolution of the spin correlation function can be described in the hydrodynamic approximation. The appropriateness of the hydrodynamic description for the transport of spin excitation in Heisenberg magnetic insulators was first pointed out by Bloembergen[3] and van Hove.[4] The idea is that for an exchange-coupled spin system obeying a Heisenberg Hamiltonian, the total spin $\vec{S}=\sum_j\vec{S}_j$ is a constant of motion. Therefore in the high-temperature limit, where no short- or long-range order is present, the microscopic spin fluctuations are governed by a diffusion equation. This means that the local two-spin correlation function $\langle S_i^\alpha(t)S_j^{\alpha\dagger}(0)\rangle$, where S_i^α is the α component of the spin at lattice site i, should be described at long times by the diffusion equation

$$D\nabla^2 g(\vec{r},t)=\frac{\partial}{\partial t}g(\vec{r},t)\,,$$

where D is the spin-diffusion coefficient and $g(\vec{r},t)$ is the correlation function for two spins at a distance r from each other. This is equivalent to say that at long times the contributions to the two-spin correlation functions

$$\langle S_i^\alpha(t) S_j^{\alpha\dagger}(0)\rangle \propto \sum_q \langle S_q^\alpha(t) S_q^{\alpha\dagger}(0)\rangle e^{i\vec{q}\cdot\vec{r}_{ij}}$$

come mainly from the long-wavelength ($q \simeq 0$) diffusive terms

$$\langle S_q^\alpha(t) S_q^{\alpha\dagger}(0)\rangle \propto e^{-Dq^2r^2t} .$$

The diffusive behavior of the spin correlation function results in dramatic effects in lower-dimensional magnetic systems. In fact a diffusive process gives a decrease of the spin correlation function as $t^{-d/2}$, where d is the dimensionality of the system. Therefore the Fourier transform of the correlation function, which defines the spectral density $f_{ij}^\alpha(\omega)$, diverges as $\omega^{-1/2}$ in 1d and as $-\ln\omega$ in 2d systems. Before mentioning the experiments which have proved the correctness of the hydrodynamic description for the high-temperature spin dynamics in a Heisenberg linear chain we would like to mention some theoretical attempts to derive the diffusive behavior from a microscopic formalism. Exact numerical calculations for finite chains (up to 11 spins for $S=\frac{1}{2}$) extrapolated to $N\to\infty$ were performed by Carboni and Richards.[5] A computer simulation of an array of 4000 spins for a classical Heisenberg linear chain was reported by Lurie, Huber, and Blume.[6] Also a theoretical analysis, based upon a two-parameter Gaussian representation of the generalized "diffusivity" was reported by Tahir-Kheli and McFadden[7] and a more complete self-consistent theoretical derivation was presented by McLean and Blume.[8] All these treatments yield basically the same results that $f_{ij}^\alpha(\omega)\to\infty$ as $\omega\to 0$, as expected from the diffusion in one dimension. The microscopic theories and the computer simulations allow one also to evaluate the diffusion coefficient D for the two-spin correlation function and the diffusion coefficient D_E for the energy correlation function.[6]

To date, the main experimental verifications of the theory are based on magnetic resonance measurements. In fact by magnetic resonance one can probe the low-frequency part of the spectral density of the spin fluctuations. Earlier EPR studies have given an indirect but striking evidence of the strong effects of spin diffusion in one dimension where deviations from Lorentzian behavior are expected.[9] First, in a study by Rogers *et al.*[10] it was found that a simple Gaussian correlation function was not able to explain the frequency dependence of the exchange-narrowed dipolar linewidth in quasi-one-dimensional copper salt $Cu(NH_3)_4SO_4\cdot H_2O$ (CTS). Later, the EPR investigation of $(CH_3)_4NMnCl_3$ (TMMC)[11] has shown deviations from Lorentzian line shape and an anomalous angular dependence of the linewidth. Both effects could be explained in terms of spin diffusion in one dimension. The function which has a diffusive behavior in the EPR case involves some four-spin correlation functions. It is the total-spin-torque correlation function (hereafter TST correlation function). The corresponding diffusion coefficient will be denoted by D_{TST}. One can point out that similar four-spin correlation functions appear in the correlation function of the exchange energy. On the other hand, from measurements of NMR spin-lattice relaxation rate one obtains directly the shape at low frequency of the spectral density of the two-spin correlation function.[12,13] The $\omega^{-1/2}$ dependence predicted by spin diffusion in one dimension was well verified by proton relaxation measurements in TMMC.[14,15]

In a "real" chain and/or for a spin Hamiltonian which is not completely isotropic, modifications in the very-long-time behavior of the correlation function are expected. In fact the $t^{-1/2}$ persistence of the correlation function due to the spin diffusion in one dimension is disrupted by a number of mechanisms. The problem can be discussed qualitatively[16] in terms of a cutoff time t_c, or a cutoff frequency ω_c, which can be defined as the time at which the $t^{-1/2}$ behavior of the spin correlation function is truncated, or the frequency at which the $\omega^{-1/2}$ divergence in the spectral density is truncated. As a consequence, the nuclear relaxation rate remains finite at low resonant frequencies and, in systems in which the cutoff frequency is large, the EPR line shape is Lorentzian like in a 3d exchange-narrowed paramagnet.

The first cutoff mechanism investigated explicitly is the mechanism involving interchain interactions[17]: the magnetic interaction of the electronic spins belonging to different chains, be it an exchange interaction or a dipolar interaction, introduces a diffusion in three dimensions and therefore limits the long-time persistence of the correlation function. Later, it has been shown that intrachain interactions can also be an important cutoff mechanism[18] since in the interaction Hamiltonian there are terms which do not commute with the total spin component and consequently the total spin is no longer a constant of motion. Finally, the presence along the magnetic chain of impurities or defects which tend to dissipate into the lattice the spin polarization could act as a cutoff mechanism.[19] However, this cutoff effect is negligible in practice because one would need a too high concentration of impurities with a very fast spin-lattice relaxation time.

The choice of TMMC for a general study of spin dynamics in Heisenberg linear chains is justified by the fact that this compound is an excellent model system; the magnetic properties are well known, the intrachain interactions are much larger than

the interchain interactions and the only nonisotropic terms in the spin Hamiltonian are the small intrachain and interchain dipolar terms.

Another important motivation for the present work relies on the results already published[15,20] which show that the cutoff frequency is strongly field dependent for some directions of the magnetic field; this is in qualitative agreement with a cutoff mechanism due to the nonsecular intrachain dipolar terms.

In this paper we present an extensive experimental and theoretical study of the high-temperature spin dynamics in TMMC. This includes (i) the analysis of the diffusive behavior of the two-spin correlation functions and their cutoff mechanisms; (ii) the analysis of the diffusive behavior of the total-spin-torque (TST) correlation function and its cutoff effects.

The theory is reformulated in more general terms taking into account the non-Markoffian feature peculiar to the hydrodynamic region in 1d systems. The connection between the cutoff process and the EPR line is clearly established. A self-consistent procedure is developed which leads to new expressions for the EPR linewidth and the cutoff frequencies due both to interchain and intrachain interactions. It is shown that from a careful analysis of the measurements of nuclear spin-lattice relaxation rates and EPR linewidth and line shape one can obtain reliable values for the diffusion coefficients D and D_{TST} and for the cutoff frequencies of the two-spin and TST correlation functions, to be compared to the theoretical calculations. For this purpose, previous measurements of T_1^{-1} and EPR have been completed and, in order to prove definitely the role of the intrachain interactions in the cutoff mechanism, measurements of $T_{1\rho}^{-1}$ have been performed.

In Sec. II we present a summary of the magnetic and structural properties of TMMC and a brief description of the experimental methods utilized. In Sec. III we summarize the theoretical expressions for the quantities which are measured and we give a detailed discussion of the calculation of the geometrical coefficients which relate the nuclear relaxation rate to the spectral densities of the electronic spin fluctuations. In Sec. IV we present the experimental results. In this section, after having introduced in the expressions for the magnetic resonance parameters the spin-diffusion coefficients D and D_{TST} and the different cutoff frequencies in a phenomenological way, we extract an "experimental" value for these quantities. In Sec. V the theory is presented and theoretical predictions are compared with the experiments while Sec. VI contains the summary and conclusions of the work.

II. SAMPLE AND EXPERIMENTAL METHODS

Tetramethyl ammonium manganese chloride $[(CH_3)_4NMnCl_3]$ provides one of the best examples of a one-dimensional Heisenberg paramagnet. The room-temperature crystal structure of TMMC was determined by Morosin and Graeber[21] and is shown in Fig. 1. The crystal structure is hexagonal with lattice constants $a = 9.151$ Å and $c' = 6.494$ Å and the space group is $P63/m$. The unit cell contains two molecules and has a center of inversion. Each molecule can be considered as made up of two ions, namely $MnCl_3^-$ and $N(CH_3)_4^+$. In a hexagonal reference system having $x \equiv a$, $y \equiv b$, and $z \equiv c$ the mirror planes are normal to the $\vec{z}$ axis and are situated at $z = \frac{1}{4}$ and $z = \frac{3}{4}$ while the manganese ions are at the origin and at $z = \frac{1}{2}$. Between two manganese ions situated along the $\vec{c}$ axis there are three chlorine ions lying on the mirror plane. These five ions form an octahedron which is slightly elongated along the $\vec{c}$ axis. The octahedra are linked to each other in chains parallel to the $\vec{c}$ axis. The tetramethyl ammonium ions are situated between the chlorines; the nitrogen atom lies on the mirror plane while the carbon atoms form a distorted tetrahedron around the nitrogen with two possible orientations of the tetrahedron both equally probable. This situation leads to a disorder in the orientation of the $(CH_3)N_4^+$ ions in the crystal. It has not been established yet if the disorder has to be regarded as static or dynamic, i.e., due to a rapid reorientation of the ion.

The static and dynamic magnetic properties of TMMC have been investigated by susceptibility,[22] specific-heat,[23] and neutron scattering measurements[24] and also by nuclear[14,15,25] and electronic magnetic resonance[11] and other techniques.[26] All

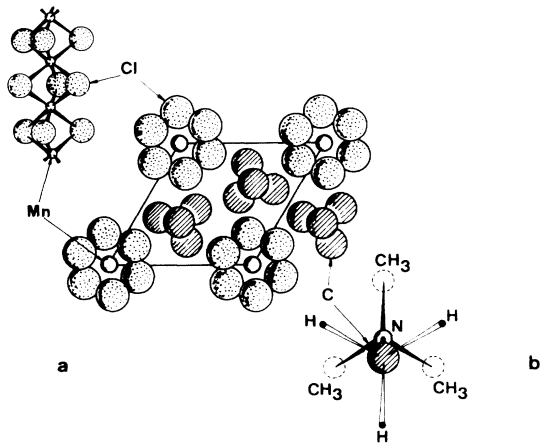

FIG. 1. Structure of TMMC (a) Chain of $MnCl_3^-$ ions and projection on the (a,b) plane; (b) model for the proton location in the $N(CH_3)_4^+$ ions.

these experiments agree on the fact that TMMC behaves like an almost ideal linear antiferromagnetic Heisenberg chain. The exchange Hamiltonian can be written

$$\mathcal{H} = -2J \sum_i \vec{S}_i \cdot \vec{S}_{i+1} ,$$

with an intrachain exchange interaction $J \simeq 6.5$ K and a Mn^{2+} magnetic moment $\mu_{eff} = g[J(J+1)]^{1/2} = 5.92$ Bohr magnetons corresponding to $g = 2$, $S = \frac{5}{2}$, and $L = 0$. The interchain interactions which lead to the three-dimensional order[23,26] at $T_N \simeq 0.8$ K are very weak.

The hyperfine interaction of the protons with the Mn^{2+} magnetic ions is predominantly dipolar. This can be understood by the fact that the protons do not participate to the $Mn^{2+} - Mn^{2+}$ exchange path and are relatively far away from the magnetic ions. The exact position of the protons in the methyl group has not been established. Some reasonable models for the proton location will be discussed in Sec. III B.

The measurements were performed on single crystals grown both at Pavia and at Grenoble. The crystals were grown by slow evaporation of an aqueous solution of equimolar manganese chloride hexahydrate and tetramethyl ammonium chloride. In some cases it was found useful to acidify the solution with 10% HCl and to use a slight excess of $MnCl_2 \cdot 6H_2O$. The typical size of the crystals is 0.5 cm^3. The $\vec{c}$ axis can be easily identified since the crystals tend to grow in the shape of roughly hexagonal prisms elongated in the direction of the chain axis $\vec{c}$.

The measurements of T_1 and $T_{1\rho}$ were performed at room temperature both at Pavia and at Grenoble using Bruker pulse spectrometers operating in the frequency range 2–100 MHz. The measurements of T_1 were performed with a 180°-90° or 90°-90° pulse sequence. The recovery of the magnetization was exponential in all cases over more than a decade. The measurements at 2 MHz done in Pavia, were performed with a Varian wide-line spectrometer by using a saturation technique. The rf calibration and the other unknown constants entering in the formula for the saturation where determined by comparing the result obtained at 4 MHz by the saturation technique with the one obtained directly by the pulse technique. These measurements were also performed by pulse techniques at St Martin d'Hères, University of Grenoble, by Chabre and Segransan. The measurements of spin-lattice relaxation in the rotating frame $T_{1\rho}$ were performed with a rf-field intensity H_1 ranging from 4 to 10 G. No dependence of $T_{1\rho}$ on the strength of H_1 was observed in the range 2–60 G. At very low rf field $T_{1\rho}$ decreases as expected when cross-relaxation effects between dipolar and Zeeman levels start playing an important role.

The EPR experiments were performed at relatively low field, the central value being $H_0 \sim 3.3$ kG. The frequency of the cavity was $\omega_e \sim 9.3$ GHz—while it was $\omega_e \sim 24$ GHz in Ref. 11. All the measurements were made with a magic tee microwave using a phase detection. The magnetic field was modulated at very low frequency (~40 Hz) with a peak-to-peak amplitude of about 30 G. For recording the EPR line the magnetic field was swept from 0 to 10 kG. The phase of the spectrometer was tuned in such a way as to get a nearly symmetrical derivative curve.

III. EXPRESSIONS FOR NUCLEAR RELAXATION RATES T_1^{-1} AND $T_{1\rho}^{-1}$ AND FOR EPR LINE

In this section we give the explicit theoretical expression for the quantities which have been measured experimentally: in Sec. III A we give the expression for T_1^{-1} and $T_{1\rho}^{-1}$ while in Sec. III C we give the expression for the EPR line. These expressions will be utilized in Sec. IV in order to extract from the experimental data the values of the quantities which characterize the electronic spin dynamics, i.e., the diffusion coefficients and the cutoff frequencies. The nuclear relaxation rate can be related to the two-spin correlation functions through geometrical coefficients which depend on the hyperfine interaction of the nuclei with the electronic spins. The precision with which one can evaluate quantitatively the relevant parameters which describe the spin dynamics is determined in a crucial way by the precision with which one can calculate the geometrical coefficients. For this reason it seems justified to include in Sec. III B a detailed discussion of the results obtained in the calculation of these coefficients in order to assess their reliability.

A. Nuclear spin-lattice relaxation rate

The dominant contribution to the spin-lattice relaxation of protons in TMMC comes from the fluctuations of the dipolar interaction which couples the nuclei with the Mn^{2+} electronic spins. The relaxation rate in the laboratory frame can be expressed in terms of the spectral densities of the electronic spin correlation functions at ω_N and at $|\omega_e \pm \omega_N| \simeq \omega_e$:

$$\frac{1}{T_1} = \sum_j \left[\Omega_1^j(\theta,\phi) f_j^z(\omega_N) + \Omega_2^j(\theta,\phi) f_j^+(\omega_e)\right] , \quad (3.1)$$

where

$$f_j^{\alpha}(\omega)=\frac{1}{2\pi}\int_{-\infty}^{+\infty} dt\, e^{i\omega t} g_j^{\alpha}(t) \qquad (3.2)$$

is the spectral density of the two-spin correlation function defined as follows:

$$g_j^{\alpha}(t)=\langle S_0^{\alpha}(t) S_j^{\alpha\dagger}(0)\rangle / \langle |S_0^{\alpha}|^2\rangle ,$$

and $f_j^{\alpha}(\omega)$ is the spectral density of

$$g_j^{\alpha}(t)=g_j^{\alpha}(t)e^{-i\omega_e t} ,$$

with $\alpha = z$ or $+$ ($\vec{z}$ axis parallel to $\vec{H}$) (referring to the longitudinal or transverse components of the electronic spin $\vec{S}$, respectively).

The corresponding expression for the relaxation rate in the rotating frame is[27]

$$\frac{1}{T_{1\rho}}=\sum_j \{\Omega_0^j(\theta,\phi) f_j^z(\omega_1)+\tfrac{1}{2}\Omega_1^j(\theta,\phi) f_j^z(\omega_N) + [\Omega_1^j(\theta,\phi)+\tfrac{1}{2}\Omega_2^j(\theta,\phi)] f_j^+(\omega_e)\} . \qquad (3.3)$$

In Eqs. (3.1) and (3.3), ω_N and ω_e are, respectively, the nuclear and electronic Larmor frequencies in the static magnetic field $\vec{H}$ while ω_1 is the nuclear Larmor frequency in the rotating rf field $\vec{H}_1$. The Ω_ξ^j's (with $\xi = 0, 1, 2$) are the usual factors associated with the dipolar couplings between protons and electrons spins.[18,20]

B. Geometrical coefficients

In the case of TMMC the positions of the protons are not exactly known. Calculations have been performed with the protons at the carbon sites.[14] Such a simplification may be justified to some extent because the methyl group rotation at high temperature results in some average of the positions. However, because of the rapid dependence of dipolar interactions with distance, we have tried to improve the model of the proton location.[15,20] The protons are certainly located on the circles which are generated by the rotation of the methyl groups around their ternary axis (the C-N bond). On these circles, we have positioned the protons in such a way that every C-H bond is in trans-position with respect to the opposite N-C bond [see Fig. 1(b)]. This assumption can be justified from steric hindrance considerations. It has also the advantage of simplicity since all the proton positions are then automatically determined.

The geometrical coefficients Ω_ξ^j have to be averaged over the three proton positions in each methyl group. The averaging is dynamical, or static, depending on whether the rotation of the methyl group is fast or slow, compared to the characteristic frequencies of the electronic-spin-fluctuations spectrum, namely the exchange frequency ω_x and the cutoff frequency ω_c, which will be discussed later. For the dynamical case, i.e., rapid motion of the protons between N sites, one has to average over the amplitudes of the couplings, while for the static case, the average has to be performed over the transition probabilities. A second averaging is necessary because of the disorder of the $N(CH_3)_4^+$ ions, which have two symmetrical configurations with respect to the mirror plane. Here again two possible cases can be considered: (i) static disorder throughout the crystal and (ii) dynamical disorder resulting from a rapid motion of inversion of the $N(CH_3)_4^+$ ions. The different possibilities have been discussed in details in Ref. 20.

In Table I we compare the different values obtained for the sums:

$$\Omega_\xi(\theta)=\sum_j \Omega_\xi^j(\theta,\phi) \quad (\text{with } \xi=0,1,2), \qquad (3.4)$$

for the two cases $\vec{H} \parallel \vec{c}$ ($\theta = 0°$) and $\vec{H} \perp \vec{c}$ ($\theta = 90°$). For a given proton we took into account the dipolar couplings with six Mn^{++} ions in each of the three nearest-neighbor chains.

It turns out that the model chosen to calculate the geometrical coefficients does not seem very crucial, except for the coefficient $\Omega_0(\theta)$, particularly for $\theta = 0$, in which case the two manners of locating the protons leads to results which are different by a factor of 3.

An important point is that the coefficient $\Omega_1(\theta)$ vanishes for $\theta = 0°$. It can be shown that, in the dynamical case, the cross terms cancel exactly the self term:

$$\sum_{j\neq 0} \Omega_1^j(\theta,\phi) = -\Omega_1^0(0°) .$$

C. Electron-paramagnetic-resonance line

In the high-temperature limit the EPR line is the spectral density $F(\omega)$ of the macroscopic two-spin correlation function

$$G(t)=\langle S^+(t) S^-(0)\rangle / \langle |S^+|^2\rangle , \qquad (3.5)$$

where S^+ represents the transverse component of the total spin:

$$S^+=\sum_{i=1}^{N} S_i^+ .$$

A very general form for $F(\omega)$ is the following:

$$F(\omega)=\frac{1}{\pi}\frac{M'(\omega)}{[\omega-\omega_e+M''(\omega)]^2+M'(\omega)^2} , \qquad (3.6)$$

where the frequency functions $M'(\omega)$ and $M''(\omega)$ defined below are related by the Kramers-Koenig relations. An alternative description for the EPR line is obtained within the Laplace transformation:

TABLE I. Values of the geometrical coefficients corresponding to the different models for the proton locations.

	Model 1 Protons at carbon sites	Model 2 Static case	Model 3 Methyl groups rotate; static disorder of $N(CH_3)_4^+$ ions	Model 4 Dynamical case: methyl groups rotate and dynamical disorder of the $N(CH_3)_4^+$ ions
$\Omega_0(0°)$	0.33		0.12	0.12
$\Omega_1(0°)$	0.013	0.009	0.004	0.000
$\Omega_2(0°)$	7.20	7.64	8.18	8.18
$\Omega_0(90°)$	1.44		2.06	2.06
$\Omega_1(90°)$	1.79	1.89	2.07	2.05
$\Omega_2(90°)$	1.98	2.00	2.18	2.15

$$\hat{F}(\omega)=\int_0^\infty dt\, e^{-i\omega t}G(t)\,, \tag{3.7}$$

and one has

$$F(\omega)=(1/\pi)\,\mathrm{Re}[\hat{F}(\omega)]\,, \tag{3.8}$$

where Re means "real part," and the frequency spectrum $\hat{F}(\omega)$ is given by

$$\hat{F}(\omega)=[i(\omega-\omega_e)+\hat{M}_0^+(\omega)]^{-1}\,, \tag{3.9}$$

with $\hat{M}_0^+(\omega)=M'(\omega)+iM''(\omega)$.

The shape and the width of $F(\omega)$ are therefore determined by the function $\hat{M}_0^+(\omega)$. In Sec. IV it will be shown that in TMMC the dominant contribution to $\hat{M}_0^+(\omega)$ comes from the fluctuations of the intrachain dipolar interactions which couple electronic spin belonging to the same chain. When the magnetic field is parallel to the chain axis ($\vec{H}\parallel\vec{c}$) one has

$$\hat{M}_0^+(\omega)\simeq\hat{M}_{0,\mathrm{intra}}^+(\omega)=3S(S+1)\omega_D^2V^2\hat{\Phi}(\omega-\omega_e)\,, \tag{3.10}$$

where $\hat{\Phi}(\omega)$ is the Laplace transform of the total spin torque (TST) correlation function. The TST correlation function involves some four-spin correlation function and will be defined explicitly in Sec. V. In Eq. (3.10) one has

$$\omega_D=\hbar\gamma_e^2/c^3\simeq 9.7\times10^9\ \mathrm{rad\ sec^{-1}}$$

and

$$V=\sum_{j(\neq i)}\left|\frac{c}{\vec{r}_{ij}}\right|^3\simeq 2.4\,,$$

where γ_e is the electron gyromagnetic ratio, c is the Mn-Mn distance along a chain, and $\vec{r}_{ij}$ is a vector joining two electron spins located on the same chain.

IV. EVALUATION OF SPIN-DIFFUSION COEFFICIENTS AND CUTOFF FREQUENCIES FROM EXPERIMENTAL RESULTS

The spectral densities of the two-spin and TST correlation functions appearing in Eqs. (3.1), (3.3), and (3.10) can be written in terms of a spin-diffusion coefficient which determines the long-time behavior of the correlation function and a cutoff frequency which limits the diffusion process in one dimension. After having presented the experimental results in Sec. IV A we show that one can extract numerical values for the diffusion coefficient and for the cutoff frequency from the nuclear magnetic relaxation (Sec. IV B) and from the EPR data (Sec. IV C).

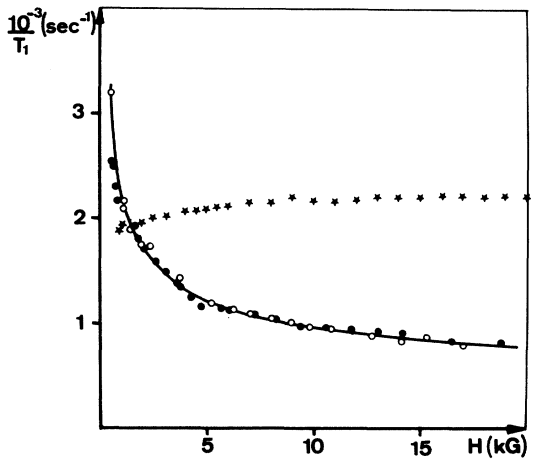

FIG. 2. Experimental proton-spin relaxation rate T_1^{-1} as a function of the applied magnetic field for $\vec{H}$ parallel and perpendicular to the chain axis. The open and black circles correspond to the measurements performed at Pavia and Grenoble, respectively.

A. Experimental results

The measurements of proton spin-lattice relaxation rate in TMMC as a function of the static magnetic field are presented in Fig. 2. These measurements were published previously and independently.[14,15] The agreement between the two sets of data obtained in different crystals is excellent. As it can be seen from Fig. 3 the T_1^{-1} results for $\vec{H} \parallel \vec{c}$ fit very well an expression of the form

$$1/T_1 = PH^{-1/2} + Q , \tag{4.1}$$

with

$$P = (6.1 \pm 0.3) \times 10^4 \ \mathrm{G}^{1/2} \mathrm{sec}^{-1} ,$$

$$Q = (3.5 \pm 0.5) \times 10^2 \ \mathrm{sec}^{-1} .$$

The results for $\vec{H} \perp \vec{c}$ show a quite different behavior, T_1^{-1} being almost constant above ~2 kG and decreasing slightly at low magnetic fields (see Fig. 2).

The measurements of proton spin-lattice relaxation rate in the rotating frame are presented in Fig. 4. The magnetic field dependence of $T_{1\rho}^{-1}$ is similar to the one observed for T_1^{-1} (see Fig. 2). In particular for $\vec{H} \parallel \vec{c}$ one can obtain a good fit with the expression

$$1/T_{1\rho} = P'H^{-1/2} + Q' , \tag{4.2}$$

with

$$P' = (3.0 \pm 0.3) \times 10^4 \ \mathrm{G}^{1/2} \mathrm{sec}^{-1} ,$$

$$Q' = (5 \pm 1) \times 10^2 \ \mathrm{sec}^{-1} ,$$

and is shown in Fig. 3.

Measurements of the absorption derivative of the EPR line at 9.3 GHz are in agreement with previous results obtained at ~24 GHz.[11,28] The half peak-to-peak derivative linewidth δH is strongly anisotropic with respect to the direction

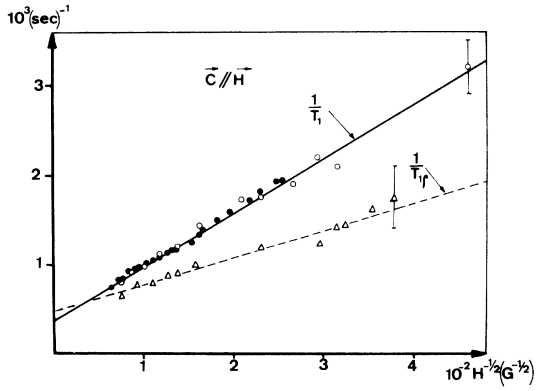

FIG. 3. Nuclear relaxation rates T_1^{-1} and $T_{1\rho}^{-1}$ as a function of $H^{-1/2}$. The straight lines correspond to Eqs. (4.1) and (4.2).

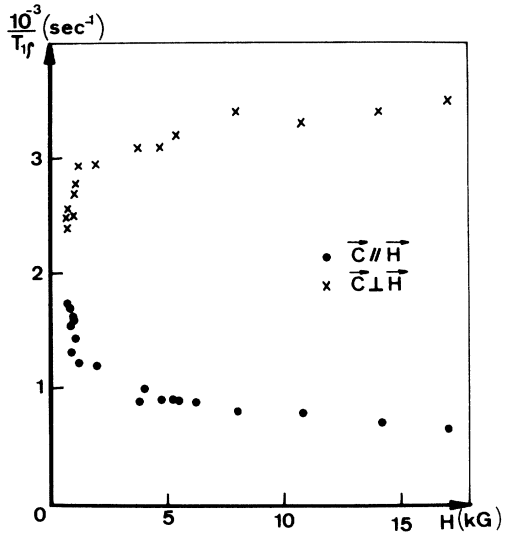

FIG. 4. Experimental proton spin-relaxation rate in the rotating frame $T_{1\rho}^{-1}$ as a function of the magnetic field for $\vec{H}$ parallel and perpendicular to the chain axis.

of $\vec{H}$. When $\vec{H}$ is parallel to the chain axis

$$\delta H \simeq 500 \ \mathrm{G} . \tag{4.3}$$

As δH is so large, the high-field resonance condition ($H_0 \gg \delta H$) cannot be completely satisfied for the low-field part of the curves. Therefore, for studying the shape of the EPR line, only the high-field region was considered, i.e., $H > H_0$. The EPR line shape is analyzed in Fig. 5 where the quantity

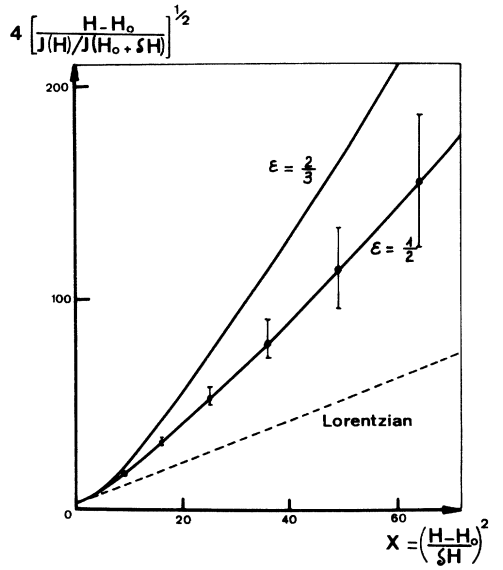

FIG. 5. Line-shape data. The full lines are theoretical curves for two values of the parameter ϵ. The dashed line corresponds to a Lorentzian EPR line.

$$Y=4\left(\frac{(H-H_0)J(H_0+\delta H)}{J(H)}\right)^{1/2} \tag{4.4}$$

is plotted versus

$$X=\left(\frac{H-H_0}{\delta H}\right)^2 .$$

The function $J(H)$ is the derivative of the absorption line at the field $H>H_0$. The straight dashed line in Fig. 5 corresponds to the case of a Lorentzian shape for which

$$Y=3+X .$$

B. Analysis of T_1, $T_{1\rho}$ data

As it has been proved experimentally and calculated theoretically, the two-spin correlation function behaves diffusively at long times. The diffusive behavior of the correlation function, which for a linear chain leads to a $t^{-1/2}$ time dependence, is valid for times longer than the exchange time τ_x and for times shorter than the cutoff time τ_c. This implies that the spectral densities $f_j^{\alpha}(\omega)$ appearing in Eqs. (3.1) and (3.3) should display a frequency dependence of the form

$$f_j^{\alpha}(\omega)\propto\omega^{-1/2}$$

in the frequency interval $\omega_c<\omega<\omega_x$. Since one finds that in TMMC $\omega_c<\omega_e<\omega_x$ one expects that $f_j^{+}(\omega_e)\propto\omega_e^{-1/2}\propto H^{-1/2}$.

Let us consider first the nuclear relaxation rate in the laboratory frame for $\vec{H}\perp\vec{c}$. In this case no contribution is expected in Eq. (3.1) from the spectral densities $f_j^{z}(\omega_N)$ since the corresponding geometrical coefficient $\Omega_1(0^\circ)$ is negligibly small. In order to explicate the expression for $f_j^{+}(\omega_e)$ we shall assume for the long-time behavior of the two-spin correlation function

$$g_j^{\alpha}(t)\simeq 1/(4\pi Dt)^{1/2} , \tag{4.5}$$

both for the auto-correlation ($j=0$) and the pair-correlation ($j=1,2,3$) functions. Thus one obtains for the spectral densities

$$\begin{aligned} f_j^{+}(\omega_e) &= 1/2\pi(2D\omega_e)^{1/2} \\ &= [1/2\pi(2D\gamma_e)^{1/2}]H^{-1/2} , \end{aligned} \tag{4.6}$$

where D is the spin-diffusion coefficient, measured in units of rad sec^{-1}, of the two-spin correlation functions. Therefore by substituting (4.6) into (3.1) one can conclude that the constant P appearing in Eq. (4.1) is given by

$$P=\Omega_1(0^\circ)/2\pi(2D\gamma_e)^{1/2} . \tag{4.7}$$

From the comparison of the theoretical expression (4.7) with the experimental value of P one can deduce the value of the spin-diffusion coefficient D, provided that the geometrical coefficients can be calculated with good accuracy. In Table II we have summarized the values that one obtains for D by using the geometrical coefficients presented in Table I which were calculated from the different models discussed in Sec. III B. The experimental value for P is 6.1×10^4 G$^{1/2}$ sec^{-1} [see Eq. (4.1)].

TABLE II. Diffusion-coefficient values obtained from T_1 and $T_{1\rho}$ data for the different proton location models.

	D (from T_1) (rad sec^{-1})	D (from $T_{1\rho}$) (rad sec^{-1})
Model 1 (H ≡ C)	$(10\pm1)\times10^{12}$	$(10.5\pm2)\times10^{12}$
Model 2 (static)	$(11.3\pm1.1)\times10^{12}$	$(12\pm2)\times10^{12}$
Model 3 (static-dynamic)	$(12.9\pm1.3)\times10^{12}$	$(13\pm2)\times10^{12}$
Model 4 (dynamic)	$(13.0\pm1.3)\times10^{12}$	$(13\pm2)\times10^{12}$

As it can be seen in Table II the values of D range from 10×10^{12} to 13×10^{12} rad sec^{-1}. The difference among the results shows that the value obtained for D is sensitive to the model chosen for the proton locations.

It should be noted that a constant term like the one observed experimentally [see Eq. (4.1)] is not present in the theoretical expression (4.6) for the spectral densities because we have considered only the diffusive part of the correlation function valid for long times. The constant term may be attributed to the short-time nondiffusive behavior of the correlation function.[14,20] However, since the constant term is small and its experimental determination is uncertain we shall not try its theoretical evaluation.

If we consider now the expression (3.3) for the relaxation rate in the rotating frame, we can see that the expression contains a contribution from the spectral density $f_j^{z}(\omega_1)$ since the corresponding geometrical coefficient is not negligible. Since $\omega_1\ll\omega_c$, one has $f_j^{z}(\omega_1)\simeq f_j^{z}(0)$. Let us assume that for $\vec{H}\parallel\vec{c}$, this term is field independent. Then from the plot of $T_{1\rho}^{-1}$ vs $H^{-1/2}$ (see Fig. 3) one can obtain an independent determination of the diffusion coefficient D. In fact the coefficient P' in Eq. (4.2) is given by

$$P'=[\Omega_1(0^\circ)+\tfrac{1}{2}\Omega_2(0^\circ)]/2\pi(2D\gamma_e)^{1/2} ,$$

and therefore from the experimental value of $P'=3\times10^4$ G$^{1/2}$ sec^{-1} one obtains the values of D listed in the last column of Table II. The agreement with the values of D obtained from T_1^{-1} measurements is very good and this confirms the as-

sumption that for $\vec{H} \| \vec{c}$ the term $f_j^z(0)$ is field independent.

In the previous part we have described the behavior at long times of the two-spin correlation function with a $(Dt)^{-1/2}$ diffusive law which is justified for an ideal Heisenberg chain. In a real Heisenberg chain the persistence at long time of the correlation function is limited by a number of possible mechanisms which will be discussed in Sec. V. Here, we limit ourselves to introduce the cutoff frequency in a phenomenological way and to show how one can determine the value of the cutoff frequency from the NMR data.

The effect of the cutoff on the spectral densities $f_j^+(\omega_e)$ is negligible since $\omega_c \ll \omega_e$. On the contrary, since $\omega_1, \omega_N \ll \omega_e$, the effect of the cutoff is very important on the spectral densities $f_j^z(\omega_N)$ and $f_j^z(\omega_1)$ which would otherwise diverge at zero frequency. Starting from the expression (4.5) for the two-spin correlation function one can introduce an abrupt cutoff at $t = \omega_c^{-1}$ and thus write

$$f_j^{\alpha}(\omega_{N,1}) = \frac{1}{\pi} \int_0^{\omega_c^{-1}} (4\pi D t)^{-1/2} \, dt = (\pi^3 D \omega_c^{\alpha})^{-1/2} . \tag{4.8}$$

A similar result is obtained by using an exponential cutoff function[16]

$$f_j^{\alpha}(\omega_{N,1}) = \frac{1}{\pi} \int_0^{\infty} (4\pi D t)^{-1/2} e^{-\omega_c^{\alpha} t} \, dt = (4\pi^2 D \omega_c^{\alpha})^{-1/2} . \tag{4.9}$$

Since the relation between $f_j^z(\omega_{N,1})$ and ω_c^z is not very sensitive to the exact form of the cutoff function, we will adopt in the following analysis the simplest model for the cutoff as expressed by Eq. (4.8).

The cutoff frequency for the case in which $\vec{H} \perp \vec{c}$ can be obtained from the T_1^{-1} measurements. In fact since $\Omega_1(0°) \sim 0$ one can use the expression (3.1) and (4.8) to obtain

$$\frac{(\omega_c^z)_{\perp}}{\omega_x} = \left[\left(T_{1\perp}^{-1} - \frac{\Omega_2(90°)}{\Omega_2(0°)} T_{1\parallel}^{-1} \right) \frac{(\pi^3 D \omega_x)^{1/2}}{\Omega_1(90°)} \right]^{-2} , \tag{4.10}$$

where $T_{1\perp}^{-1}$ and $T_{1\parallel}^{-1}$ refer, respectively, to the relaxation rate for $\vec{H} \perp \vec{c}$ and $\vec{H} \| \vec{c}$. We have normalized the cutoff frequency to the exchange frequency ω_x, which is defined as

$$\omega_x = J[\tfrac{8}{3} z S(S+1)]^{1/2}, \tag{4.11}$$

where z is the number of nearest neighbors. In TMMC, $J/k \simeq 6.5$ K (Ref. 21) and therefore $\omega_x \simeq 6 \times 10^{12}$ rad sec^{-1}. One can obtain an independent determination of $\omega_{c\perp}^z (\vec{H} \perp \vec{c})$ by using the experimental data for T_1^{-1} and $T_{1\rho}^{-1}$. From Eqs. (3.1), (3.3), and (4.8) one has

$$\frac{(\omega_c^z)_{\perp}}{\omega_x} = \left[\left(T_{1\rho\perp}^{-1} - \tfrac{1}{2} T_{1\perp}^{-1} - \frac{\Omega_1(90°)}{\Omega_2(0°)} T_{1\parallel}^{-1} \right) \frac{(\pi^3 D \omega_x)^{1/2}}{\Omega_0(90°)} \right]^{-2} . \tag{4.12}$$

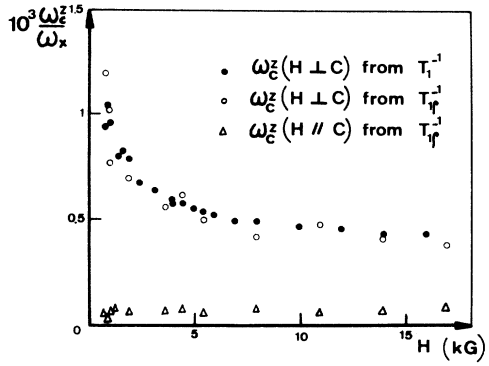

FIG. 6. Experimental cutoff frequency ω_c^z as a function of the field for $\vec{H}$ parallel and perpendicular to the chain axis.

The values of ω_c^z will depend on the model adopted for the proton location since the geometrical coefficients and the experimental value for D depend on the choice of the model.

The values of the cutoff frequency for $\vec{H} \perp \vec{c}$ obtained from Eq. (4.10) and the experimental data of Eq. (4.2) are practically independent from the model adopted for the proton location. These values of ω_c^z are plotted in Fig. 6. On the other hand the values obtained for $(\omega_c^z)_{\perp}$ $(\vec{H} \perp \vec{c})$ from Eq. (4.12) depend very much on the model adopted for the geometrical coefficients. By adopting the geometrical coefficients pertaining to model 3 or model 4 (see Table I) one finds for $(\omega_c^z)_{\perp}$ values which are in good agreement with the one obtained from Eq. (4.10) and the data of T_1^{-1}. The models 1 and 2 instead would lead to values smaller by a factor of three. This fact represents a strong argument in favour of the adoption of model 3 or model 4 for the location of the protons and also a confirmation that the procedure adopted for the evaluation of $(\omega_c^z)_{\perp}$ is quite reliable.

As seen in Fig. 6 the cutoff frequency $(\omega_c^z)_{\perp}$ is field dependent with a divergence at low fields. In Fig. 6 it can be seen that the values of $(\omega_c^z)_{\perp}$ fit well a law of the type

$$(\omega_c)_{\perp}/\omega_x = A + BH^{-1/2}, \tag{4.13}$$

with

$$A = (2.2 \pm 0.4) \times 10^{-4} ,$$

$$B = (240 \pm 50) \times 10^{-4} \text{ G}^{-1/2} .$$

As it will be shown in Sec. V the field-dependent part of the cutoff frequency for $\vec{H} \perp \vec{c}$ is explicitly given by

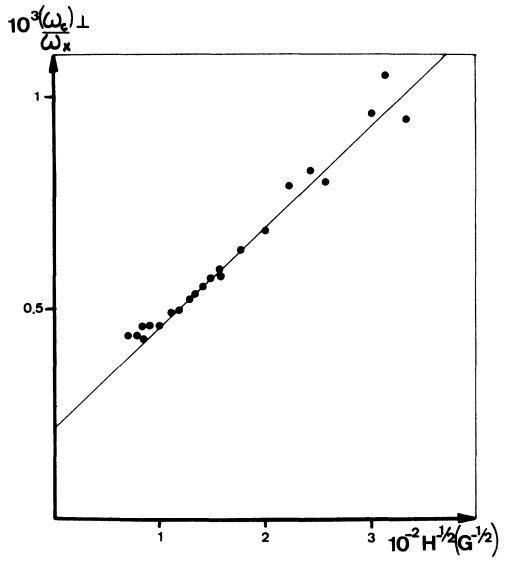

FIG. 7. Experimental cutoff frequency $(\omega_c^z)_\perp$ as a function of $H^{-1/2}$. The straight line corresponds to Eq. (4.13).

$$(\omega_c^z)_\perp = 3S(S+1)\omega_D^2 V^2 \,\mathrm{Re}[\hat{\Phi}(2\omega_e)]\,,$$

where $\hat{\Phi}(\omega)$ is the spectral density of the TST correlation function [see Eq. (3.10)]. Therefore the $H^{-1/2}$ dependence found gives evidence for the diffusive behavior of the TST correlation function. (See Fig. 7.) Then, by giving to $\hat{\Phi}(\omega)$ the following diffusive law:

$$\hat{\Phi}(\omega) = 1/(4D_{\mathrm{TST}}\, i\omega)^{1/2}\,, \tag{4.14}$$

Eq. (4.13) allows an experimental determination for D_{TST}. We obtain

$$D_{\mathrm{TST}} \simeq (3.7 \pm 1.5)\times 10^{13}\ \mathrm{rad\,sec^{-1}}\,.$$

The determination of the cutoff frequency for the case in which $\vec{H} \| \vec{c}$ is more uncertain. In fact, since $\Omega_1(0°) \simeq 0$, the cutoff frequency for $\vec{H} \| \vec{c}$ appears only in the expression for $T_{1\rho\|}^{-1}$. Furthermore, even in the expression for $T_{1\rho\|}^{-1}$ [see Eq. (3.3)], the geometrical coefficient $\Omega_0(0°)$ is small. From Eqs. (3.1), (3.3), and (4.8) one obtains

$$\frac{(\omega_c^z)_\|}{\omega_x} = \left((T_{1\rho\|}^{-1} - \tfrac{1}{2}T_{1\|}^{-1}) \frac{(\pi^3 \omega_x D)^{1/2}}{\Omega_0(0°)} \right)^{-2}\,. \tag{4.15}$$

The important feature of the results shown in Fig. 6 is that, while the cutoff frequency for $\vec{H} \perp \vec{c}$ displays a strong field dependence, the values of $(\omega_c^z)_\|$ are almost independent of the magnetic field H. One has $(\omega_c^z)_\|/\omega_x \simeq 10^{-4}$. We can note that this value is of the same order of magnitude as the value of A in Eq. (4.13). The implications of these results are discussed in Sec. VI.

C. Analysis of EPR data

For interpreting EPR data in 1d Heisenberg systems, a diffusive behavior has been assumed also for the TST correlation function.[11,29] For $\omega = 0$, the function $\hat{\Phi}(\omega)$ expressed in Eq. (4.14) exhibits a divergence. In order to remove it, the following more realistic description will be used:

$$\hat{\Phi}(\omega) = 1/[4D_{\mathrm{TST}}(i\omega + \Gamma)]^{1/2}\,, \tag{4.16}$$

where the constant Γ plays the role of a cutoff frequency, and its physical meaning will be discussed in Sec. V.

Expression (4.16) defines completely the EPR line by means of the two parameters D_{TST} and Γ which can be determined experimentally since two independent quantities are accessible from EPR experiments. One is given directly by the linewidth ΔH. The second one comes from the non-Lorentzian line shape. By using Eq. (4.16) for $\hat{\Phi}(\omega)$ in the evaluation of the EPR line shape, one obtains that the quantity Y [Eq. (4.4)] depends only on the parameter

$$\epsilon = 3S(S+1)\omega_D^2 V^2/\Gamma(4\Gamma D_{\mathrm{TST}})^{1/2}\,. \tag{4.17}$$

In Fig. 5, two curves are drawn for different values of ϵ. The curve with $\epsilon = 0.5$ fits the experimental data fairly well. For this value of ϵ the "reduced" peak-to-peak linewidth of $J(H)$ is given by

$$\gamma_e \delta H/\Gamma = 0.46\,. \tag{4.18}$$

From the experimental values $\epsilon = 0.5$ and $\delta H = 500$ G one gets from Eqs. (4.17) and (4.18)

$$\begin{aligned} &D_{\mathrm{TST}} = (2.9 \pm 0.7)\times 10^{13}\ \mathrm{rad\,sec^{-1}}\,, \\ &\Gamma \simeq (1.9 \pm 0.4)\times 10^{10}\ \mathrm{rad\,sec^{-1}}\,. \end{aligned} \tag{4.19}$$

It is interesting to note that the value of Γ is quite comparable with the half linewidth ΔH at half power of the EPR absorption line. For $\epsilon = 0.5$ one has $\Delta H/\delta H \sim 1.3$, and then

$$\gamma_e \Delta H \simeq 1.14\times 10^{10}\ \mathrm{rad\,sec^{-1}}\,.$$

D. Summary of experimental results

In the previous paragraphs we have proved the diffusive behavior of the two-spin and TST correlation functions from the analysis of the field dependence of the nuclear T_1 and $T_{1\rho}$ and of the EPR line. These diffusive behaviors are characterized by diffusion coefficients D and D_{TST}, respectively, and by corresponding cutoff frequencies ω_c and Γ. The experimental values obtained for these parameters are summarized in Table III, where $[\omega_c(\infty)]_\perp$ is the infinite field extrapolation for the cutoff frequency [see the term A in Eq.

TABLE III. Recapitulation of the experimental results: D and D_{TST} are the diffusion coefficients of the two-spin and TST correlation function, respectively; $(\omega_c^g)_{\parallel}$ is the cutoff frequency of the longitudinal two-spin correlation function for $\vec{H} \parallel \vec{c}$; $[\omega_c^g(\infty)]_{\perp}$ is the extrapolated value for $\vec{H} \perp \vec{c}$; Γ is the cutoff frequency of the TST correlation function, and ΔH is the EPR linewidth.

D/ω_x	D_{TST}/ω_x	$(\omega_c^g)_{\parallel}$	$[\omega_c^g(\infty)]_{\perp}$	Γ	$\gamma_e \Delta H$
2.2 ± 0.2 (T_1)	6.2 ± 2.5 (T_1)	0.6×10^9 rad sec^{-1}	1.3×10^9 rad sec^{-1}	1.9×10^{10} rad sec^{-1}	1.14×10^{10} rad sec^{-1}
2.2 ± 0.4 ($T_{1\rho}$)	4.8 ± 1.2 (EPR)				

(4.13)].

One should point out that the values for D correspond to model 3 or 4 and the uncertainty takes into account only the $T_{1,1\rho}$ measurement imprecision. In particular, the uncertainties coming from the J value and from the fact that the proton locations are unknown have been ignored. For D_{TST} the values obtained by T_1^{-1} and EPR measurements should be considered in agreement, taking into account the experimental uncertainty attached to their evaluation. Furthermore we would like to draw the attention on the following points: the ratio between D_{TST} and D is of the order of 2, the values of $(\omega_c^g)_{\parallel}$ and $[\omega_c^g(\infty)]_{\perp}$, relative to the cutoff process for the two-spin correlation function, are of the same order of magnitude; the same is true for the quantities Γ and $\gamma_e \Delta H$.

V. THEORETICAL DESCRIPTION OF SPIN DYNAMICS INCLUDING INTRACHAIN AND INTERCHAIN DIPOLAR INTERACTIONS AND COMPARISON WITH EXPERIMENTAL RESULTS

The two-spin correlation functions $g_j^{\alpha}(t)$ involved in the expressions of T_1^{-1} and $T_{1\rho}^{-1}$ will be described in terms of the expectation values of the fluctuations of the spin-wave vector:

$$S_q^{\alpha} = N^{-1/2} \sum_{i=1}^{N} S_i^{\alpha} e^{-i \vec{q} \cdot \vec{r}_i} , \tag{5.1}$$

so that

$$g_{j=0}^{\alpha}(t) = \sum_q g_q^{\alpha}(t) ,$$

with

$$g_q^{\alpha}(t) = \langle S_q^{\alpha}(t) S_q^{\alpha\dagger}(0) \rangle / \langle |S_q^{\alpha}|^2 \rangle .$$

In these expressions, the time modulation of the spin operators $S_q^{\alpha}(t)$ is governed by the following Hamiltonian:

$$\mathcal{H} = \omega_e S^z + \mathcal{H}_{SS} ,$$

expressed in units of rad sec^{-1}. The first term is the Zeeman interaction and $\mathcal{H}_{SS}$ represents the spin-spin couplings. The latter is the sum of four terms

$$\mathcal{H}_{SS} = \mathcal{E} + \mathfrak{D} + e + d .$$

(i) $\mathcal{E}$ is the intrachain Heisenberg Hamiltonian

$$\mathcal{E} = -2J \sum_i \vec{S}_i \cdot \vec{S}_{i+1} .$$

(ii) $\mathfrak{D}$ represents the intrachain dipolar interactions. The secular part is given by

$$\mathfrak{D}_0 = \tfrac{1}{4}(1 - 3\cos^2\theta)\omega_D \sum_{i \neq j} \left(\frac{c}{r_{ij}}\right)^3 (3 S_i^z S_j^z - \vec{S}_i \cdot \vec{S}_j) ;$$

and the nonsecular parts are

$$\mathfrak{D}^{\pm 1} = -\tfrac{3}{4} \sin\theta \cos\theta e^{\mp i\phi} \omega_D \sum_{i \neq j} \left(\frac{c}{r_{ij}}\right)^3 \times (S_i^z S_j^{\pm} + S_i^{\pm} S_j^z) ,$$

$$\mathfrak{D}^{\pm 2} = -\tfrac{3}{8} \sin^2\theta e^{\mp 2i\phi} \omega_D \sum_{i \neq j} \left(\frac{c}{r_{ij}}\right)^3 S_i^{\pm} S_j^{\pm} ,$$

where θ and ϕ are the polar angles defining the orientation of the vector $\vec{r}_{ij}$ which joins two electronic spins on the same chain—i.e., defining the orientation of the $\vec{c}$ axis—in the reference system having the $\vec{z}$ axis along the magnetic field $\vec{H}$.

(iii) e represents the interchain Heisenberg hamiltonian

$$e = -J' \sum_{i,j} \vec{S}_i \cdot \vec{S}_j .$$

In this expression, the spins $\vec{S}_i$ and $\vec{S}_j$ are located on different chains and the coupling J' connects only the nearest spins.

(iv) d represents the interchain dipolar interactions. The secular and nonsecular parts are, respectively,

$$d^0 = \tfrac{1}{4}\omega_d \sum_{i,j} A_{ij}^0 (3 S_i^z S_j^z - \vec{S}_i \cdot \vec{S}_j) ,$$

$$d^{\pm 1} = -\tfrac{3}{4}\omega_d \sum_{i,j} A_{ij}^{\pm 1}(S_i^z S_j^{\pm} + S_i^{\pm} S_j^z),$$

$$d^{\pm 2} = -\tfrac{3}{8}\omega_d \sum_{i,j} A_{ij}^{\pm 2} S_i^{\pm} S_j^{\pm},$$

with

$$A_{ij}^0 = (1 - 3\cos^2\theta_{ij})(a/r_{ij})^3,$$
$$A_{ij}^{\pm 1} = \sin\theta_{ij}\cos\theta_{ij} e^{\mp i\phi_{ij}}(a/r_{ij})^3,$$
$$A_{ij}^{\pm 2} = \sin^2\theta_{ij} e^{\mp 2i\phi_{ij}}(a/r_{ij})^3,$$

where θ_{ij} and ϕ_{ij} are the polar angles defining the orientation of the vector $\vec{r}_{ij}$ which joins two electronic spins belonging to different chains in the same reference system as previously. The distance between two neighboring chains is a and

$$\omega_d = \hbar\gamma_e^2/a^3 \simeq 4.26\times 10^8 \text{ rad sec}^{-1}.$$

In TMMC, one expects the interchain Heisenberg interactions to be very small. By assuming that the three-dimensional order at $T_N \sim 0.8$ K is only due to the interchain Heisenberg couplings, an evaluation of J' would give $J' \simeq 3\omega_d$.[22]

For systems of spins coupled predominantly by Heisenberg interactions, many derivations of the wave-vector correlation function $f_q^{\alpha}(t)$ have been proposed. The first descriptions were of Markoffian type. Such descriptions lead to a Lorentzian shape for the spectral density. Basically they rely on the assumption that the fluctuations of the torque dS_q^{α}/dt are definitely faster than the characteristic time of the fluctuations of $S_q^{\alpha}(t)$. In other words, possible memory effects are neglected. Such is the Kubo-Tomita[30] derivation of the EPR line. For pure Heisenberg systems the spin-diffusion theory of Mori and Kawasaki,[31] for instance, relies also on such a fast-torque-fluctuation assumption. In three-dimensional systems these descriptions are very successful as the fast-torque-fluctuation assumption is correct, at least if only diffusive modes, i.e., those associated with small values of the vector $\vec{q}$, are considered. In the general case, more sophisticated derivations have to be used which precisely take into account the memory effects.[32-34]

In one-dimensional systems, the EPR line is observed to have a characteristic non-Lorentzian shape. This has to be understood as a consequence of memory effects attributable to the long persistence of the microscopic fluctuations. The specific problem of the EPR line in TMMC is studied in details in another paper[29] where the "memory function" is calculated following the projection operator technique proposed by Mori[35] and developed recently by Reiter.[36] In Appendix A we present a different derivation which has the advantage of expressing the memory effects in terms of the correlation function of the torque dS_q^{α}/dt so that the connection with the previous Markoffian descriptions can easily be made. The result is that in the Laplace representation [Eq. (3.7)] the frequency spectrum of $g_q^{\alpha}(t)$ may be expressed as follows:

$$\hat{f}_q^{\alpha}(\omega) = [i(\omega - n_{\alpha}\omega_e) + \hat{M}_q^{\alpha}(\omega)]^{-1}, \tag{5.2}$$

where the memory spectrum $\hat{M}_q^{\alpha}(\omega)$ is given by

$$\hat{M}_q^{\alpha}(\omega) = -i(\omega - n_{\alpha}\omega_e)\frac{C_q^{\alpha} + i\hat{T}_q^{\alpha}(\omega)}{\omega - n_{\alpha}\omega_e + C_q^{\alpha} + i\hat{T}_q^{\alpha}(\omega)}, \tag{5.3}$$

with

$$C_q^{\alpha} = \langle [\mathcal{H}_{SS}, S_q^{\alpha}] S_q^{\alpha\dagger}\rangle / \langle |S_q^{\alpha}|^2\rangle.$$

In Eqs. (5.2) and (5.3), $n_{\alpha} = 0$ for $\alpha = z$ and $n_{\alpha} = 1$ for $\alpha = +$. The function $\hat{T}_q^{\alpha}(\omega)$ is the Laplace transform of the torque correlation function

$$T_q^{\alpha}(t) = \langle e^{i\mathcal{H}t}[\mathcal{H}_{SS}, S_q^{\alpha}] e^{-i\mathcal{H}t}[S_q^{\alpha\dagger}, \mathcal{H}_{SS}]\rangle / \langle |S_q^{\alpha}|^2\rangle. \tag{5.4}$$

Equation (5.3) gives an exact expression for $\hat{M}_q^{\alpha}(\omega)$. Let us note that as long as $|\omega - n_{\alpha}\omega_e| \gg |C_q^{\alpha} + i\hat{T}_q^{\alpha}(\omega)|$, $\hat{M}_q^{\alpha}(\omega)$ can be approximated as

$$\hat{M}_q^{\alpha}(\omega) \simeq -iC_q^{\alpha} + \hat{T}_q^{\alpha}(\omega).$$

The first term C_q^{α} gives a shift of the central frequency of the mode q, which vanishes at infinite temperature. Therefore one has

$$\hat{M}_q^{\alpha}(\omega) \simeq \hat{T}_q^{\alpha}(\omega) \tag{5.5}$$

for

$$|\omega - n_{\alpha}\omega_e| \gg |\hat{T}_q^{\alpha}(\omega)| \quad \text{at } T \to \infty.$$

A. EPR line (mode $q = 0$)

The EPR frequency spectrum $\hat{F}(\omega)$ [Eq. (3.9)] describes the mode $q = 0$ of the transverse spin component ($\alpha = +$). Therefore Eq. (5.2) leads to

$$\hat{F}(\omega) = \hat{f}_{q=0}^{+}(\omega) = [i(\omega - \omega_e) + \hat{M}_0^{+}(\omega)]^{-1}.$$

As $[S^+, \mathcal{S}] = 0$ the paramagnetic shift C_0^+ of the EPR line is just given by

$$C_0^+ = \langle [\mathfrak{D}, S^+] S^-\rangle / \langle |S^+|^2\rangle$$

(the interchain dipolar contribution is definitely much smaller). The quantity C_0^+ has been shown to be quite negligible in TMMC at room temperature.[37] Hence Eq. (5.3) becomes

$$\hat{M}_0^{+}(\omega) = (\omega - \omega_e)\hat{T}_0^{+}(\omega)/[\omega - \omega_e + i\hat{T}_0^{+}(\omega)].$$

For calculating $\hat{M}_0^{+}(\omega)$ we shall consider separately the "high"- and "low"-frequency regions

defined by the conditions $|\omega-\omega_e| \gg |\hat{T}_0^+(\omega)|$ and $|\omega-\omega_e| \lesssim |\hat{T}_0^+(\omega)|$, respectively. Physically, the high-frequency region corresponds to the wings of the EPR line ($|\omega-\omega_e| \gg \gamma_e \Delta H$) while the low-frequency region describes its central part ($|\omega-\omega_e| \lesssim \gamma_e \Delta H$).

In the high-frequency region, Eq. (5.5) can be used. Hence

$$\hat{M}_0^+(\omega) \simeq \hat{T}_0^+(\omega) .$$

An additional approximation can also be made concerning $T_0^+(t)$: one can neglect the influence of the dipolar terms $(\mathfrak{D}+d)$ upon the modulation of $T_0^+(t)$. One can write

$$T_0^+(t) \simeq \langle e^{i\mathcal{H}'t}[\mathcal{H}_{SS}, S_{q=0}^+]e^{-i\mathcal{H}'t}[S_{q=0}^-, \mathcal{H}_{SS}]\rangle / \langle |S_{q=0}^+|^2\rangle , \tag{5.6}$$

with

$$\mathcal{H}' = \omega_e S^z + \mathcal{E} + e .$$

This means that in the wings of the EPR line, the behavior of $F(\omega)$ displays the spin fluctuations of a quasipure Heisenberg system. This basical feature also comes up in the Kubo-Tomita formalism.

1. Intrachain dipolar interaction

The main contribution to $T_0^+(t)$ comes from the intrachain dipolar interactions. (It will be shown that the interchain dipolar interactions give to the EPR line a very negligible contribution.) Hence for $\mathcal{H}_{SS}=\mathfrak{D}$ in Eq. (5.6) one obtains:

$$T_{0,\text{intra}}^+(t) = \Phi(t)e^{i\omega_e t}[F_0^2(\theta) + F_1^2(\theta)(3e^{-i\omega_e t} + 2e^{i\omega_e t}) + F_2^2(\theta)e^{-2i\omega_e t}] , \tag{5.7}$$

where

$$F_0^2(\theta) = \tfrac{3}{4}S(S+1)(1-3\cos^2\theta)^2\omega_D^2 V^2 ,$$

$$F_1^2(\theta) = \tfrac{3}{2}S(S+1)\sin^2\theta\cos^2\theta\,\omega_D^2 V^2 ,$$

$$F_2^2(\theta) = \tfrac{3}{4}S(S+1)\sin^4\theta\,\omega_D^2 V^2 ,$$

and where $\Phi(t)$ is the TST correlation function explicitly given by

$$\Phi(t) = V^{-2}N^{-1}\sum_{i\neq j}\sum_{l\neq m}\left|\frac{c}{r_{ij}}\right|^3\left|\frac{c}{r_{lm}}\right|^3 \times \frac{\langle e^{i\mathcal{E}t}S_i^+S_j^+e^{-i\mathcal{E}t}S_l^-S_m^-\rangle}{\frac{8}{9}[S(S+1)]^2} . \tag{5.8}$$

In the modulation of $\Phi(t)$ the interchain Heisenberg Hamiltonian e has been neglected. First, let us recall that Eq. (5.8) is only valid in the wings of the EPR line, i.e., for $t \ll (\Delta H)^{-1}$ and that the EPR linewidth is originated from the intrachain dipolar interactions. Then, since in TMMC $J' \ll \omega_D$ we expect the role of e to be negligible in the evolution of $\Phi(t)$ in the wings of the EPR line. In Eq. (5.7) use has been made of the relations given by Carboni and Richards [Eq. (46) in Ref. 5] which express the rotationally invariant property of the four-spin correlation functions at infinite temperature.

For $\vec{H} \| \vec{c}$ ($\theta = 0°$) expression (5.7) is reduced to

$$T_{0,\text{intra}}^+(t) = F_0^2(0°)\Phi(t)e^{i\omega_e t} . \tag{5.9}$$

The diffusive law attributed in Sec. IV to $\hat{\Phi}(\omega)$ for interpreting the frequency dependence of $(\omega_c^z)_\perp$ and for interpreting the EPR line shape allows one to write

$$\Phi(t) = 1/(4\pi D_{\text{TST}}t)^{1/2} , \tag{5.10}$$

where D_{TST} is the diffusion coefficient of the TST correlation function.

In the low-frequency region, i.e., for $|\omega-\omega_e| \lesssim |\hat{T}_0^+(\omega)|$ the description of the memory function of the EPR line is definitely more difficult. Such an attempt has recently been made by using a self-consistent description.[29] Here we simply propose to limit the diffusion of $\Phi(t)$ by introducing a cutoff function such as

$$\Phi(t) \to \Phi(t)e^{-\Gamma t} .$$

The corresponding memory spectrum becomes

$$\hat{M}_{0,\text{intra}}^+(\omega) = F_0^2(0°)\hat{\Phi}(\omega-\omega_e) , \tag{5.11}$$

with

$$\hat{\Phi}(\omega) = 1/[4D_{\text{TST}}(i\omega+\Gamma)]^{1/2} . \tag{5.12}$$

Rigorously Γ in Eq. (5.12) is frequency dependent. However for the purpose of studying the diffusive behavior of the TST correlation function $\Phi(t)$ the frequency-independent cutoff approximation is quite sufficient since it gives the correct behavior in the wings of the EPR line. On the other hand, this approximation leads to a qualitative but convenient definition for Γ as being the cutoff frequency of the memory function. From the qualitative argument that the memory function of a correlation function cannot last longer than the function itself, it seems reasonable to write for the EPR line

$$\Gamma^{-1} \lesssim (\gamma_e \Delta H)^{-1} .$$

Moreover, as previously for the two-spin correlation function the different cutoff mechanisms to be considered are related to the interchain interaction and/or those interactions which break the spherical symmetry of the Heisenberg Hamiltonian $\mathcal{E}$. In our case, the former are negligible and the latter are the intrachain dipolar interactions which gives also the EPR linewidth ΔH.

Therefore one expects that Γ would be rather of the order of $\gamma_e \Delta H$. Such a value is precisely what we obtain in the interpretation of Sec. IV (see Table III). This experimental agreement reinforces our euristic argument, explicitly expressed as $\Gamma \simeq \gamma_e \Delta H$. Hence a theoretical evaluation for ΔH can be obtained from Eq. (5.11):

$$\gamma_e \Delta H = \mathrm{Re}[\hat{M}^+_{0,\mathrm{intra}}(\omega_e + \gamma_e \Delta H)] , \tag{5.13}$$

and one gets the self-consistent equation

$$\gamma_e \Delta H \simeq 0.78 F_0^2(0^\circ)/(4 D_{\mathrm{TST}} \gamma_e \Delta H)^{1/2} , \tag{5.14}$$

which leads to

$$\gamma_e \Delta H \simeq 0.85\, F_0(0^\circ)[F_0(0^\circ)/4 D_{\mathrm{TST}}]^{1/3} . \tag{5.15}$$

A theoretical calculation of $\Phi(t)$ has been performed by using the q-mode decoupling approximation for the four-spin correlation functions.[29] Then, by using a diffusive law for the two-spin correlation function, one gets

$$\Phi(t) = 1/[4\pi(2D)t]^{1/2} . \tag{5.16}$$

The comparison with Eq. (5.10) shows that the independent q-mode approximation predicts the diffusion coefficient D_{TST} of the TST correlation function to be twice the diffusion coefficient D of the two-spin correlation functions. This result seems to be quite consistent with our experimental determinations (see Table III).

2. *Interchain dipolar interactions*

We now consider the contribution to $T_0^+(t)$ of the interchain dipolar interactions d. As previously, the short- and long-time behavior will be studied separately.

For example, for the secular term d^0 [$\mathcal{H}_{SS} = d^0$ in Eq. (5.6)] the short-time behavior is given by

$$T^+_{0,\mathrm{inter}}(t) = \tfrac{9}{4}\omega_d^2 \frac{1}{N} \sum_{i,j} \sum_{l,m} A^0_{ij} A^0_{lm} \times \frac{e^{i\omega_e t}\langle e^{i\mathcal{S}t} S^z_i S^+_j e^{-i\mathcal{S}t} S^-_l S^z_m \rangle}{\langle |S^+_0|^2 \rangle} . \tag{5.17}$$

There, the spins $\vec{S}_i$ and $\vec{S}_j$, $\vec{S}_l$ and $\vec{S}_m$ belong to different chains and therefore an exact decoupling becomes possible. The four-spin correlation functions in Eq. (5.17) can be written

$$\langle e^{i\mathcal{S}t} S^z_i S^+_j e^{-i\mathcal{S}t} S^-_l S^z_m \rangle = \langle e^{i\mathcal{S}t} S^z_i e^{-i\mathcal{S}t} S^z_m \rangle_\mu \langle e^{i\mathcal{S}t} S^+_j e^{-i\mathcal{S}t} S^-_l \rangle_\nu ,$$

where μ and ν label different chains. For $\omega_x t \gg 1$ each term of the product behaves diffusively:

$$\langle e^{i\mathcal{S}t} S^z_i e^{-i\mathcal{S}t} S^z_m \rangle \propto (4\pi D t)^{-1/2} \exp\left(-\frac{r^2_{im}/c^2}{4Dt}\right) .$$

In this expression, the exponential factor takes into account the fact that the two spins $\vec{S}_i$ and $\vec{S}_m$ are separated by the distance $|\vec{r}_{im}|$ on the same chain μ. A similar factor comes up for the spins $\vec{S}_j$ and $\vec{S}_l$ of the chain ν. The sum over all the indices in Eq. (5.17) attributes to these exponential factors an important role which results in giving the torque function $T^+_{0,\mathrm{inter}}(t)$ again a linear diffusive law, the diffusion coefficient being exactly 2D.[38] For the full dipolar interchain Hamiltonian the complete expression is given by

$$T^+_{0,\mathrm{inter}}(t) = \Psi(t) e^{i\omega_e t}[F'^2_0(0^\circ) + F'^2_1(0^\circ)(3e^{-i\omega_e t} + 2e^{+i\omega_e t}) + F'^2_2(0^\circ) e^{-2i\omega_e t}] ,$$

with

$$F'^2_0(0^\circ) = \tfrac{9}{2} S(S+1)\omega_d^2 \left| \sum_i^\mu A^0_{ij} \right|^2 ,$$

$$F'^2_1(0^\circ) = 9 S(S+1)\omega_d^2 \left| \sum_i^\mu A^{\pm 1}_{ij} \right|^2 ,$$

$$F'^2_2(0^\circ) = \tfrac{9}{2} S(S+1)\omega_d^2 \left| \sum_i^\mu A^{\pm 2}_{ij} \right|^2 ,$$

and

$$\Psi(t) = 1/[4\pi(2D)t]^{1/2} . \tag{5.18}$$

In conclusion, by summing the interaction couplings over an infinite number of spins along each chain, taking into account the intrachain pair-correlation terms, one is led to the noticeable result that $\Psi(t)$ is also diffusive. Therefore, in nearly 1d systems, also the interchain dipolar interactions can be in principle responsible for giving a non-Lorentzian shape to the EPR line. However, another important feature results from this calculation which shows that among the different interchain dipolar terms, when the magnetic field is parallel to the chain axis, only the nonsecular term d^{-2} leads to a non negligible contribution. For the secular term d^0, the sum of the geometrical coefficients in $F'^2_0(0^\circ)$ over all the spins i of the chain μ is very small and negligible (this sum is exactly zero if a continuous integration is used). For the nonsecular terms $d^{\pm 1}$, the corresponding sum involved in $F'^2_1(0^\circ)$ is exactly zero for reasons of symmetry. For d^{-2}, the sum over the geometrical coefficients in $F'^2_2(0^\circ)$ is $\sum_i^\mu A^{\pm 2}_{ij} \simeq 3.76$, and one gets

$$F'^2_2(0^\circ) \simeq 10^{20} \ (\mathrm{rad\,sec^{-1}})^2 .$$

This term adds to the memory spectrum $\hat{M}^+_0(\omega)$ a contribution which is approximately a constant when the magnetic field H is swept around H_0. This can be evaluated by considering, as done previously, that the long-time behavior of $\Psi(t)$ is described

by a cutoff function $\exp(-\Gamma t)$ with $\Gamma \simeq \gamma_e \Delta H$. This procedure leads to

$$\hat{M}^{+}_{0,\text{inter}}(\omega) = F_2'^2(0^\circ)\,\hat{\Psi}(\omega - \omega_e + 2\omega_e)\,,$$

where

$$\hat{\Psi}(\omega) = 1/[8D(i\omega + \gamma_e \Delta H)]^{1/2}\,.$$

By assuming $|\omega - \omega_e| \simeq \gamma_e \Delta H \ll \omega_e$, one gets

$$\mathrm{Re}[\hat{M}^{+}_{0,\text{inter}}(\omega_e)] = F_2'^2(0^\circ)/4(2D\omega_e)^{1/2}\,,$$

which evaluates the interchain nonsecular contribution to the EPR linewidth ΔH. By using for D the experimental value for the diffusion coefficient (see Table III) and for $H = 3$ kG we obtain $\Delta H \simeq 1.2$ G. The comparison with the experimental value $\delta H \simeq 500$ G leads to the conclusion that the interchain dipolar interactions are quite negligible for the EPR line in TMMC.

B. Diffusive modes ($q \neq 0$)

For describing modes for which the vector $\vec{q}$ is different from zero but small ($q_z c \ll 1$) we shall follow the same "self-consistent" procedure as developed previously for the EPR line ($q = 0$). The high-frequency region of the mode, i.e., $|\omega - n_\alpha \omega_e| \gg \delta^\alpha(q)$, where

$$\delta^\alpha(q) = \mathrm{Re}\{\hat{M}^{+}_{q}[n_\alpha \omega_e + \delta^\alpha(q)]\}$$

represents the width of the mode q, is first considered. For this region which corresponds to the wings of the mode q, the expression for the torque correlation function can be written

$$T^\alpha_q(t) \simeq \langle e^{i\mathcal{H}'t}[\mathcal{H}_{SS}, S^\alpha_q]\, e^{-i\mathcal{H}'t}[S^{\alpha\dagger}_q, \mathcal{H}_{SS}]\rangle / \langle |S^\alpha_q|^2\rangle\,, \tag{5.19}$$

with $\mathcal{H}' = \omega_e S^z + \mathcal{E}$. Again, the dipolar and interchain Heisenberg terms are neglected upon the time modulation of $T^+_q(t)$ as in Eq. (5.6). Then the central part of the q mode, i.e., for $|\omega - n_\alpha \omega_e| \lesssim \delta^\alpha(q)$, is described by introducing a cutoff function in $T^\alpha_q(t)$

$$T^\alpha_q(t) \to T^\alpha_q(t) e^{-\Gamma t}\,.$$

By Laplace transforming this expression one obtains the memory spectrum $\hat{M}^\alpha_q(\omega)$ of the q mode. Finally, the self-consistent feature of this procedure is achieved by writing that the cutoff Γ is of the order of the linewidth $\delta^\alpha(q)$ of the q mode.

Since $\mathcal{H}_{SS} = \mathcal{E} + \mathfrak{D} + e + d$, the memory spectrum is the sum of three terms

$$\hat{M}^\alpha_q(\omega) = \hat{M}^\alpha_{q,\text{Heis}}(\omega) + \hat{M}^\alpha_{q,\text{intra}}(\omega) + \hat{M}^\alpha_{q,\text{inter}}(\omega)\,, \tag{5.20}$$

corresponding to the intrachain Heisenberg, the intrachain dipolar, and the interchain interactions, respectively.

1. *Heisenberg interaction: diffusion coefficient*

The Heisenberg Hamiltonian $\mathcal{E}$ is expected to yield the diffusive character of the spin system. Different derivations have been given for the diffusion coefficient D which is defined by

$$\hat{M}^\alpha_{q,\text{Heis}}(\omega \to 0) = D q_z^2 c^2\,.$$

In Refs. 7 and 11 a Gaussian shape was assumed *a priori* for $T^\alpha_{q,\text{Heis}}(t)$ [$\mathcal{H}_{SS} = \mathcal{E}$ in Eq. (5.19)]. This calculation has been improved first by considering higher-order moments in the description of the short-time part of this function ($\omega_x t \lesssim 1$).[39] Second, we have treated the long-time part in the q-mode decoupling approximation. This procedure leads to a self-consistent equation for D which is solved for the value $D/\omega_x \simeq 0.91$.[38] Compared with the simple Gaussian description this value can be considered as a net improvement (+42%) but it is smaller than the experimental value. Our results and different theoretical determinations of D/ω_x are listed in Table IV.

2. *Intrachain dipolar interaction*

Let us consider the expression of $T^+_{q,\text{intra}}(t)$ for the secular term $\mathfrak{D}^0$ [$\mathcal{H}_{SS} = \mathfrak{D}^0$ and $\alpha = +$ in Eq. (5.19)]:

$$T^+_{q,\text{intra}}(t) = V^{-2} F_0^2(\theta) N^{-1} \sum_{\substack{i \neq j \\ l \neq m}} \left|\frac{c}{r_{ij}}\right|^3 \left|\frac{c}{r_{lm}}\right|^3 \times \cos\vec{q}\cdot\vec{r}_{jm}\, \frac{\langle e^{i\mathcal{H}'t} S^z_i S^+_j e^{-i\mathcal{H}'t} S^z_l S^-_m\rangle}{\frac{8}{9}[S(S+1)]^2}\,.$$

Since the spins S_j and S_m are on the same chain, only the q_z component enters in this expression. On the other hand in the expansion of the cosine function the lowest-order term corresponds to the value $q_z = 0$. Therefore one can write

$$T^+_{q,\text{intra}}(t) \simeq T^+_{0,\text{intra}}(t) + O(q_z^2 c^2)\,,$$

where $T^+_{0,\text{intra}}(t)$ corresponds precisely to the case of the EPR line [Eq. (5.7)]. For $q_z c \ll 1$ the higher-order terms $O(q_z^2 c^2)$ can be neglected in comparison with the $q_z^2 c^2$ contribution of the Heisenberg term. Therefore, for $\vec{H} \| \vec{c}$ ($\theta = 0^\circ$) the expression for $\hat{M}^+_{q,\text{intra}}(\omega)$ is obtained directly from Eqs. (5.11) and (5.12) in which the cutoff Γ is to be replaced by $\delta^\alpha(q)$. One obtains

$$\hat{M}^+_{q,\text{intra}}(\omega) \simeq \hat{M}^+_{0,\text{intra}}(\omega) = F_0^2(0^\circ)\hat{\Phi}^+_q(\omega - \omega_e)\,, \tag{5.21}$$

with

$$\hat{\Phi}^\alpha_q(\omega) = 1/\{4D_{\text{TST}}[i\omega + \delta^\alpha(q)]\}^{1/2}\,.$$

For $\alpha = z$, a similar analysis can be developed, and we get

$$T^z_{q,\text{intra}}(t) \simeq T^z_{0,\text{intra}}(t)\,,$$

TABLE IV. Comparison of the different theoretical values of the diffusion coefficient D with the experimental determination.

	Gaussian approximation	Present model	Theory of McLeane and Blume (Ref. 8)	Computer simulation (Ref. 6)	Experiment (see Table III)
$S=\infty$	0.63		1.20	1.3 ± 0.1	
$S=\frac{5}{2}$	0.64	0.91			2.2 ± 0.2

where

$$T^z_{0,\text{intra}}(t)=\Phi(t)[F_1^2(\theta)(e^{-i\omega_e t}+e^{i\omega_e t}) + 2F_2^2(\theta)(e^{-2i\omega_e t}+e^{2i\omega_e t})]. \quad (5.22)$$

It should be pointed out that only the nonsecular terms $\mathfrak{D}^{\pm1}$ and $\mathfrak{D}^{\pm2}$ enters in $T^z_q(t)$. The secular term $\mathfrak{D}^0$ does not play any role for the very reason that S^z_q commutes with the part $\sum_{ij}S^z_iS^z_j$ of the Hamiltonian. The Heisenberg part of $\mathfrak{D}^0$ adds only a negligible contribution to the diffusion coefficient D. Consequently, for $\theta=0^0$ ($\vec{H}\|\vec{c}$) one has

$$T^z_{0,\text{intra}}(t)=0\,. \quad (5.23)$$

There is no contribution to the memory spectrum coming from the intrachain dipolar interactions.

For $\theta=90°$ ($\vec{H}\perp\vec{c}$) one obtains from Eq. (5.22)

$$\hat{M}^z_{0,\text{intra}}(\omega)=2F_2^2(90°)[\hat{\Phi}^z_q(\omega-2\omega_e)+\hat{\Phi}^z_q(\omega+2\omega_e)]\,. \quad (5.24)$$

3. *Interchain dipolar interactions: e + d*

Finally, we have to consider the interchain interactions. The Heisenberg and dipolar Hamiltonian will be treated together. Two kinds of terms which play different roles have to be distinguished in $T^\alpha_q(t)$. Some are associated with the transverse components q_x and q_y of the wave vector $\vec{q}$. They provide a three-dimensional character to the dynamical process. The others depend only on the parallel component q_z. For these terms the main contribution is independent of the q_z value. As in the case of the intrachain dipolar interactions it corresponds to $q_z=0$.[38] We present here the result concerning the $\alpha=z$ component which is the only case of interest, especially since for $\theta=0°$ the intrachain contributions are zero [see Eq. (5.23)]. Because of the specific properties already noted about the geometrical coefficients $\sum_j^\mu A^\eta_{ij}$ ($n=0$, $\pm1,\pm2$) when $\vec{H}\|\vec{c}$, we can write

$$T^z_{q,\text{inter}}(t)=\Psi(t)[\alpha(q_x,q_y)\omega_x'^2 + \beta(q_x,q_y)F_2'^2(0°)(e^{i\omega_e t}+e^{-i\omega_e t})], \quad (5.25)$$

where $\omega_x'=4J'[S(S+1)]^{1/2}$ is the characteristic frequency of the Heisenberg interchain interaction and

$$\alpha(q_x,q_y)=\tfrac{1}{3}\{(1-\cos q_x a)+[1-\cos(q_x\tfrac{1}{2}a+q_y a\tfrac{1}{2}\sqrt{3})] + [1-\cos(q_x\tfrac{1}{2}a-q_y a\tfrac{1}{2}\sqrt{3})]\},$$

$$\beta(q_x,q_y)=\tfrac{1}{3}\{(1+\cos q_x a)+[1+\cos(q_x\tfrac{1}{2}a+q_y a\tfrac{1}{2}\sqrt{3})] + [1+\cos(q_x\tfrac{1}{2}a-q_y a\tfrac{1}{2}\sqrt{3})]\}.$$

The corresponding expression for the memory spectrum is given by

$$\hat{M}^z_{q,\text{inter}}(\omega)=\alpha(q_x,q_y)\omega_x'^2\hat{\Psi}^z(\omega)+\beta(q_x,q_y)F_2'^2(0°) \times[\hat{\Psi}^z(\omega+2\omega_e)+\hat{\Psi}^z(\omega-2\omega_e)]\,, \quad (5.26)$$

with

$$\hat{\Psi}^z_q(\omega)=1/\{8D[i\omega+\delta^z(q)]\}^{1/2}\,. \quad (5.27)$$

C. Two-spin correlation functions

In this paragraph we establish the expression for the quantities which are connected with the experimental data. The expressions for T_1^{-1} and $T_{1\rho}^{-1}$ depend explicitly on the spectral densities $f^z(\omega_N)$ and $f^+(\omega_e)$. From the definitions (3.2) and (3.7) one has

$$f^\alpha(\omega)=(2\pi)^{-1}[\hat{f}^\alpha(\omega)+\hat{f}^{\alpha*}(\omega)], \quad (5.28)$$

and $\hat{f}^\alpha(\omega)$ is related to the spectral density of the q modes by

$$\hat{f}^\alpha(\omega)=\sum_q\hat{f}^\alpha_q(\omega)\,. \quad (5.29)$$

As we are interested in the very-low-frequency behavior of $f^\alpha(\omega)$, only diffusive modes will be considered in the sum of Eq. (5.29). Furthermore $\hat{f}^\alpha(\omega_N)\sim\hat{f}^\alpha(0)$ since $\omega_N\ll\omega_c,\omega_e,\omega_x$. First, we shall deal with the case of pure diffusion. Then we shall consider disturbance from the 1d diffusion by intra- and interchain interactions.

1. *Pure diffusion*

For $\alpha=+$ and $\vec{H}\|\vec{c}$ ($\theta=0°$), one obtains from Eqs. (5.2) and (5.20)

$$\hat{f}^+(0)=\sum_q\frac{1}{-i\omega_e+Dq_z^2c^2+\hat{M}^+_{0,\text{intra}}(0)}=\hat{f}^+(\omega_e)\,, \quad (5.30)$$

where the interchain contribution to $\hat{M}_q^+(\omega)$ has been neglected. The intrachain contribution is obtained from Eq. (5.21):

$$\hat{M}^+_{0,\,\mathrm{intra}}(0)=\frac{F_0^2(0^\circ)}{[4D_{\mathrm{TST}}(-i\omega_e+\delta^+(q))]^{1/2}}, \tag{5.31}$$

where the width $\delta^+(q)$ of the q mode is given by the definition

$$\delta^+(q)=\mathrm{Re}\{\hat{M}_q^+(\omega_e+\delta^+(q))\},$$

which in the present case is reduced to

$$\delta^+(q)=Dq_z^2c^2+\mathrm{Re}\{\hat{M}^+_{0,\,\mathrm{intra}}(\omega_e+\delta^+(q))\}.$$

Before going further in the calculation of Eq. (5.30) an important remark is in order about the expression to be considered effectively for $\delta^+(q)$. As long as q_z is such that $Dq_z^2c^2 \gg \mathrm{Re}[\hat{M}^+_{0,\,\mathrm{intra}}(0)]$, the term $\hat{M}^+_{0,\,\mathrm{intra}}(0)$ is quite negligible in Eq. (5.30) and the expression for $\delta^+(q)$ does not matter really. On the other hand, for $Dq_z^2c^2 \ll \mathrm{Re}[\hat{M}^+_{0,\,\mathrm{intra}}(0)]$ the diffusive term $Dq_z^2c^2$ can be neglected in the expression of $\delta^+(q)$ itself, more especially as

$$\mathrm{Re}[\hat{M}^+_{0,\,\mathrm{intra}}(0)]<\mathrm{Re}\{\hat{M}^+_{0,\,\mathrm{intra}}[\omega_e+\delta^+(q)]\}.$$

Therefore, it seems appropriate to define an effective cutoff frequency by

$$\delta^+_{\mathrm{eff}}(q)=\mathrm{Re}\{\hat{M}^+_{0,\,\mathrm{intra}}[\omega_e+\delta^+_{\mathrm{eff}}(q)]\}, \tag{5.32}$$

and also quite sufficient to use this expression instead of $\delta^+(q)$ in Eq. (5.31). From Eq. (5.21) one gets the explicit expression

$$\delta^+_{\mathrm{eff}}(q)=\frac{0.78F_0^2(0^\circ)}{4D_{\mathrm{TST}}\delta^+_{\mathrm{eff}}(q)},$$

which displays the self-consistent feature of the present description and which establishes that the effective cutoff for the TST correlation function is the EPR linewidth [compare with Eq. (5.14)]

$$\delta^+_{\mathrm{eff}}(q)=\gamma_e\Delta H.$$

Consequently, $\hat{M}^+_{0,\,\mathrm{intra}}(0)$ does not depend on q_z and, since it is just a constant in the sum of Eq. (5.30), its real part plays the role of the cutoff frequency for the two-spin correlation function $f^+(\omega)$

$$(\omega_c^+)_{\parallel}=\mathrm{Re}[\hat{M}^+_{0,\,\mathrm{intra}}(0)],$$

and one gets

$$(\omega_c^+)_{\parallel}=\mathrm{Re}\left(\frac{F_0^2(0^\circ)}{[4D_{\mathrm{TST}}(-i\omega_e+\gamma_e\Delta H)]^{1/2}}\right).$$

This cutoff frequency is field dependent, and we note that for $H=0$ it is of the order of $\gamma_e\Delta H$ [see Eq. (5.14)]. However, for $\omega_e>\gamma_e\Delta H$ its value decreases rapidly, and in Eq. (5.30) the term $\hat{M}^+_{0,\,\mathrm{intra}}$ becomes negligible. Hence, $f^+(\omega_e)$ behaves practically according to a pure diffusive law:

$$f^+(\omega_e)=1/2\pi(2D\omega_e)^{1/2}.$$

This explains why experimentally any cutoff effect was not observed on $T_{1\parallel}^{-1}\propto f^+(\omega_e)$.

2. *Intrachain cutoff*

For $\alpha=z$ and $\vec{H}\perp\vec{c}$ ($\theta=90^\circ$), again the interchain part is negligible in Eq. (5.20), and from Eq. (5.2) we can write

$$\hat{f}^z(0)=\sum_q\frac{1}{Dq_z^2c^2+\hat{M}^z_{0,\,\mathrm{intra}}(0)}.$$

The expression for $\hat{M}^z_{0,\,\mathrm{intra}}(0)$ is obtained from Eq. (5.24). One gets

$$\hat{M}^z_{0,\,\mathrm{intra}}(0)=\mathrm{Re}\left(\frac{F_2^2(90^\circ)}{\{4D_{\mathrm{TST}}[2i\omega_e+\delta^z(q)]\}^{1/2}}\right), \tag{5.33}$$

where we may assume that the cutoff $\delta^z(q)$ is much smaller than $2\omega_e$ and negligible. The expression of $\hat{M}^z_{0,\,\mathrm{intra}}(0)$ becomes independent on q_z and, therefore, represents the cutoff frequency $(\omega_c^z)_\perp$ for $f^z(\omega)$. From Eq. (5.33) one can write

$$\frac{(\omega_c^z)_\perp}{\omega_x}=\frac{F_2^2(90^\circ)}{\omega_x(D_{\mathrm{TST}}\omega_e)^{1/2}}.$$

This cutoff is field dependent, and its behavior displays the diffusive law of the TST correlation function. It is precisely the experimental result reported in Sec. IV.

3. *Interchain cutoff*

For $\alpha=z$ and $\vec{H}\parallel\vec{c}$ ($\theta=0^\circ$) only the intrachain Heisenberg and the interchain Hamiltonians contribute to $\hat{M}_q^z(\omega)$. One has

$$\hat{f}^z(0)=\sum_q\frac{1}{Dq_z^2c^2+\hat{M}^z_{q,\,\mathrm{inter}}(0)}. \tag{5.34}$$

The expression for $\hat{M}^z_{q,\,\mathrm{inter}}(0)$ will be obtained from Eq. (5.26). For evaluating the cutoff $\delta^z(q)$ which enters in the function $\hat{\Psi}^z(\omega)$ [Eq. (5.27)] the analysis previously developed for $\delta^+(q)$ can be repeated here, leading to the following definition for the effective cutoff frequency:

$$\delta^z_{\mathrm{eff}}(q)=\mathrm{Re}\{\hat{M}^z_{q,\,\mathrm{inter}}[\delta^z_{\mathrm{eff}}(q)]\}.$$

This equation allows first a self-consistent determination of $\delta^z_{\mathrm{eff}}(q)$ from Eq. (5.26)

$$\delta^z_{\mathrm{eff}}(q)=0.78\frac{\alpha(q_x,q_y)\omega_x'^2}{[8D\delta^z_{\mathrm{eff}}(q)]^{1/2}}+\frac{\beta(q_x,q_y)F_2'^2(0^\circ)}{(8D\omega_e)^{1/2}}, \tag{5.35}$$

and also to rewrite Eq. (5.34) as

$$\hat{f}^z(0)=\sum_q\frac{1}{Dq_z^2c^2+\delta^z_{\mathrm{eff}}(q)}. \tag{5.36}$$

Furthermore, we note that if $\delta^z_{\rm eff}(q)$ depends on the transverse component q_x and q_y it does not depend on q_z. Therefore, this quantity will lead to a cutoff effect on the 1d diffusive behavior of $f^z(\omega)$. After integration over q_z in Eq. (5.36) and by use of Eq. (5.28) one gets

$$f^z(0)=\frac{1}{\pi}\sum_{q_x,q_y}\frac{1}{[4D\delta^z_{\rm eff}(q)]^{1/2}}\,.$$

The comparison with Eq. (4.9) where an exponential cutoff function is used leads for the cutoff frequency $(\omega^z_c)_{\parallel}$ to the following expression:

$$\frac{(\omega^z_c)_{\parallel}}{\omega_x}=\left[\sum_{q_x,q_y}\left(\frac{\omega_x}{\delta^z_{\rm eff}(q)}\right)^{1/2}\right]^{-2}.$$

This cutoff is field dependent. However its behavior expresses the diffusive law of the two-spin correlation functions. In high field, a constant contribution remains, which comes from the first term in Eq. (5.35). For this part, a numerical determination gives

$$\frac{(\omega^z_c)_{\parallel}}{\omega_x}\simeq 0.53\,\frac{\omega'_x}{\omega_x}\left(\frac{\omega'_x}{8D}\right)^{1/3}.$$

By using for D and $(\omega^z_c)_{\parallel}$ the experimental values given in Table III, one can determine the interchain Heisenberg coupling

$$J'\simeq 17\times 10^8\ \text{rad sec}^{-1}$$

or

$$J'/k\simeq 1.3\times 10^{-2}\ \text{K}\,.$$

VI. SUMMARY AND CONCLUSION

The main feature of the high-temperature spin dynamics in 1d Heisenberg system is the diffusive behavior of the microscopic fluctuations, which for the corresponding correlation functions results in a divergence of the spectral densities as $\omega\to 0$. Indeed such a behavior was already recognized for both the two-spin and the TST correlation functions, but here we have presented an attempt of a purely experimental determination of the corresponding diffusion coefficients D and $D_{\rm TST}$, respectively. This study has been performed on TMMC which is an excellent 1d Heisenberg model system of spins $S=\frac{5}{2}$. For D, two independent determinations whose the values agree fairly well (see Table II) have been obtained from the field dependence of the proton relaxation times T_1 and $T_{1\rho}$. In fact, the experimental value for D depends strongly, within 30%, on the model chosen for the location and the motion of the protons. However, the further analysis of the experimental results concerning the cutoff effects tends to show that the most reliable value for D corresponds to the models which take into account the geometry of the methyl groups and their possible motion (models 3 and 4 in Table II). For $D_{\rm TST}$, also independent determinations have been obtained. One results directly from the analysis of the EPR line and the others from the analysis of the field dependence of T_1^{-1} and $T_{1\rho}^{-1}$ at very low magnetic field, which was interpreted in terms of cutoff mechanisms.

Basically our experimental method stems from an exhaustive analysis of the different cutoff mechanisms which may limit the divergence of the spectral densities $f^{\alpha}(\omega)$ of the two-spin correlation functions. In particular, the role of the intrachain and interchain dipolar interactions have been analyzed in great detail. First, for the intrachain dipolar interactions, we have established formally that they lead to cutoff effects. We have shown that for $f^z(\omega)$ the corresponding cutoff frequency ω^z_c is directly related to the EPR linewidth ΔH. In fact, ω^z_c and $\gamma_e\Delta H$ are both the width of the uniform mode ($q=0$), but associated with the parallel and transverse spin components (S^z and S^+), respectively. Since S^z commutes with the secular term $\mathfrak{D}^0$, ω^z_c, unlike $\gamma_e\Delta H$, depends only on the nonsecular terms of the intrachain dipolar interactions. For this reason, one can actually compare ω^z_c to the part of the EPR linewidth which corresponds to the so-called "$\frac{10}{3}$ effect." The field and angular dependences of the two quantities are the same. The field dependence reproduces the frequency dependence of the TST correlation function and the angular dependence predicts that ω^z_c is to be maximum for $\vec{H}\perp\vec{c}$ and exactly zero for $\vec{H}\parallel\vec{c}$. Experimentally we can consider that the correctness of this description has been proved since: (i) a diffusive law $H^{-1/2}$ is actually observed for $(\omega^z_c)_{\perp}$ as expected from the diffusive behavior of the TST correlation function; (ii) the two values for the diffusion coefficient $D_{\rm TST}$ obtained from T_1 and EPR measurements compare well (see Table III); and (iii) for $\vec{H}\parallel\vec{c}$ the cutoff frequency is definitely smaller than for the other directions of the field and is almost constant: $(\omega^z_c)_{\parallel}$ can be interpreted in terms of interchain cutoff mechanisms. It has been shown from geometrical considerations, specific to 1d Heisenberg systems, that the interchain dipolar contribution to $(\omega^z_c)_{\parallel}$ is quite negligible in TMMC. As a consequence, the interchain cutoff effect has been attributed to Heisenberg interactions. From the experimental determination of $(\omega^z_c)_{\parallel}$ a value has been obtained for the interchain exchange integral, $J'\simeq 17\times 10^8$ rad sec^{-1}. This is four times the value of the interchain dipolar coupling ω_d, in agreement with the evaluation of the interchain effective fields from the Néel temperature presented in Ref. 22. In addition, it should be noted that the values for $(\omega^z_c)_{\parallel}$ and the

infinite field extrapolation $[\omega_c^z(\infty)]_\perp$ are of the same order of magnitude (see Table III). Because of the diffusive field dependence of the intrachain dipolar cutoff frequency, one can expect that the intrachain contribution to $(\omega_c^z)_\perp$ becomes negligible for $H \to \infty$. Hence, the remaining contribution should come from the interchain interactions, and this explains the comparable values observed for $(\omega_c^z)_\parallel$ and $[\omega_c^z(\infty)]_\perp$.

The theoretical derivation that we have presented for describing the diffusive q modes refers to the language of non-Markoffian processes where the memory function plays an essential role. In 1d Heisenberg systems such a description is quite appropriate, particularly for the mode for which a non-negligible part of the width $\delta^\alpha(q)$ is given by the cutoff frequency ω_c^α: $\delta^\alpha(q) \simeq Dq_z^2c^2 + \omega_c^\alpha$. In this case, the memory function of the mode behaves at long times according to a 1d diffusive law, no matter if the cutoff mechanism is generated from the intra- or interchain dipolar interactions, the corresponding diffusion coefficient being D_{TST} or $2D$. The resulting long persistence of the memory function may last up to times of the order of the inverse of the width $[t \lesssim \delta^{\alpha-1}(q)]$ and cause a deformation in the shape of the mode which is no longer Lorentzian: such an effect is directly observed on the EPR line. A precise description of the memory function at $t > \delta^{\alpha-1}(q)$ is certainly a difficult problem. However, one knows intuitively that a cutoff mechanism will short circuit the 1d diffusive law, and since we are only interested in an evaluation for ω_c^α we have used the simplest description giving an exponential law to the cutoff function of the memory function: $e^{-\Gamma t}$. The crucial point is rather in the value of Γ. The expectation that Γ is to be of the order of the width of the mode is confirmed experimentally since, for the EPR line, we obtained $\Gamma \simeq \gamma_e \Delta H$. In fact this situation corresponds to the limiting case when the EPR linewidth ΔH and the cutoff frequency Γ are generated from the same interactions, i.e., the intra- and interchain dipolar interactions in the present case. In the more general case, an extra cutoff mechanism may be due to some interchain Heisenberg interactions and the cutoff frequency Γ is larger than $\gamma_e \Delta H$. For strong interchain Heisenberg couplings, one may have $\Gamma \gg \gamma_e \Delta H$ and the EPR line becomes again Lorentzian. However, the interchain Heisenberg interactions are smaller in TMMC. As a consequence of the value of Γ, the theoretical procedure that we have developed presents an evident self-consistent feature which we made use of for getting compact expressions not only for the EPR linewidth but also for the intra- and interchain cutoff frequencies. Our expression for the EPR linewidth [Eq. (5.14)] is slightly different from the expression previously given for 1d Heisenberg system[11] and leads to smaller value for $\Delta H (\sim -30\%)$. On the other hand, concerning the intra- and interchain cutoff effects, the present derivation is the first treatment which takes into account the dipolar interactions.

Concerning the experimental results for D and D_{TST} reported in Table III, we would like first to point out that their relative values are consistent with the theoretical expectation obtained when the decoupling procedure is used for treating the four-spin correlation functions, namely $D_{\mathrm{TST}}/D = 2$. Recently, the simulation techniques have shown that for 1d Heisenberg systems of "classical" spins $(S \to \infty)$, one observes the same ratio between the energy diffusion coefficient D_E and D,[6] and this result agrees also with the expectation of the decoupling procedure. Then, at this stage of the discussion it is worth drawing again the attention on the very consistent feature displayed by all the results of the present experimental study. Certainly, this consistency is the strongest argument in favor of the chosen value for the diffusion coefficient, $D \simeq 13 \times 10^{12}$ rad sec^{-1}, despite of the uncertainty on the exact model for the protons. This value is surprisingly much larger than any theoretical expectation (see Table IV). It is almost a factor of 2 greater than the result given by the simulation technique which corresponds to $S \to \infty$.[40] One possible cause of the discrepancy might be the spin value which is $S = \frac{5}{2}$ instead of ∞ as in simulation methods. Repeating for $S > \frac{5}{2}$, the calculation of the diffusion coefficient developed in Sec. V, one actually obtains smaller values for D/ω_x. However the difference is only of few percent, and we may expect that it would be the same in any improved description. Therefore, one is led to seek for another explanation which could be simply that the value of the exchange integral could be larger than $J/k \sim 6.5$ K. By using the values $D/\omega_x = 1.3$ corresponding to $S \to \infty$ and $D = 13 \times 10^{12}$ rad sec^{-1} one obtains $J/k \simeq 10$ K. One should note that the value $J/k \simeq 7.7$ K was used for interpreting neutron data.[24]

ACKNOWLEDGMENTS

The authors are greatly indebted to Y. Barjhoux and F. Ferrieu for the computation help and to P. Baladda for preparation of samples. Stimulating discussions with Professor P. M. Richards are also gratefully acknowledged. One of us (J-P. B.) would like to thank Professor V. Jaccarino for the opportunity to perform part of this work at Santa Barbara. He would also like to thank Dr. A. R. King and E. Dormann for their help in the EPR experiments.

APPENDIX A: GENERAL EXPRESSION FOR $\hat{f}_q^{\alpha}(\omega)$

Here, we present a derivation for $\hat{f}_q^{\alpha}(\omega)$, the Laplace transform of

$$g_q^{\alpha}(t) = \langle S_q^{\alpha}(t) S_q^{\alpha\dagger} \rangle / \langle |S_q^{\alpha}|^2 \rangle .$$

From the equation of motion of $S_q^{\alpha}(t)$

$$\frac{d}{dt} S_q^{\alpha}(t) = i n_{\alpha} \omega_e S_q^{\alpha}(t) + i e^{i\mathcal{H}t} [\mathcal{H}_{SS}, S_q^{\alpha}] e^{-i\mathcal{H}t} , \tag{A1}$$

where $\mathcal{H} = \omega_e S^z + \mathcal{H}_{SS}$, and where $\mathcal{H}_{SS}$ represents the Hamiltonian for the spin-spin interactions [cf. Eq. (5.3)] the evolution of $\langle S_q^{\alpha}(t) S_q^{\alpha\dagger} \rangle$ is readily obtained to be

$$\frac{d}{dt} \langle S_q^{\alpha}(t) S_q^{\alpha\dagger} \rangle = i n_{\alpha} \omega_e \langle S_q^{\alpha}(t) S_q^{\alpha\dagger} \rangle + i \langle e^{i\mathcal{H}t} [\mathcal{H}_{SS}, S_q^{\alpha}] e^{-i\mathcal{H}t} S_q^{\alpha\dagger} \rangle . \tag{A2}$$

In the following, we will use the Laplace transformation:

$$\hat{f}(\omega) = \int_0^{\infty} dt\, e^{-i\omega t} g(t) , \tag{A3}$$

which yields a convenient frequency description. One defines

$$\langle\langle S_q^{\alpha} | S_q^{\alpha\dagger} \rangle\rangle_{\omega} = \int_0^{\infty} dt\, e^{-i\omega t} \langle S_q^{\alpha}(t) S_q^{\alpha\dagger} \rangle .$$

With the transformation (A3), Eq. (A2) is changed into

$$i(\omega - n_{\alpha}\omega_e) \langle\langle S_q^{\alpha} | S_q^{\alpha\dagger} \rangle\rangle_{\omega} = \langle S_q^{\alpha} S_q^{\alpha\dagger} \rangle + i \langle\langle [\mathcal{H}_{SS}, S_q^{\alpha}] | S_q^{\alpha\dagger} \rangle\rangle_{\omega} . \tag{A4}$$

This expression can also be written in the following form:

$$\langle\langle S_q^{\alpha} | S_q^{\alpha\dagger} \rangle\rangle_{\omega} = \langle |S_q^{\alpha}|^2 \rangle / [i(\omega - n_{\alpha}\omega_e) + \hat{M}_q^{\alpha}(\omega)] , \tag{A5}$$

with

$$\hat{M}_q^{\alpha}(\omega) = -i \langle\langle [\mathcal{H}_{SS}, S_q^{\alpha}] | S_q^{\alpha\dagger} \rangle\rangle_{\omega} / \langle\langle S_q^{\alpha} | S_q^{\alpha\dagger} \rangle\rangle_{\omega} . \tag{A6}$$

An alternative expression corresponding to (A5) can be given for Eq. (A2):

$$\frac{d}{dt} \langle S_q^{\alpha}(t) S_q^{\alpha\dagger} \rangle = i n_{\alpha} \omega_e \langle S_q^{\alpha}(t) S_q^{\alpha\dagger} \rangle - \int_0^t d\tau\, m_q^{\alpha}(\tau) \langle S_q^{\alpha}(t-\tau) S_q^{\alpha\dagger} \rangle . \tag{A7}$$

$m_q^{\alpha}(t)$ is called the memory function, and the Laplace transform of $m_q^{\alpha}(t)$ is precisely $\hat{M}_q^{\alpha}(\omega)$:

$$\hat{M}_q^{\alpha}(\omega) = \int_0^{\infty} dt\, e^{-i\omega t} m_q^{\alpha}(t) .$$

For the numerator of Eq. (A6) one can write an equation of motion similar to Eq. (A4):

$$i(\omega - n_{\alpha}\omega_e) \langle\langle [\mathcal{H}_{SS}, S_q^{\alpha}] | S_q^{\alpha\dagger} \rangle\rangle_{\omega} = \langle [\mathcal{H}_{SS}, S_q^{\alpha}] S_q^{\alpha\dagger} \rangle + i \langle\langle [\mathcal{H}_{SS}, S_q^{\alpha}] | [S_q^{\alpha\dagger}, \mathcal{H}_{SS}] \rangle\rangle_{\omega} . \tag{A8}$$

Inserting Eqs. (A8) and (A4) in Eq. (A6) then leads for $\hat{M}_q^{\alpha}(\omega)$ to the following expression:

$$\hat{M}_q^{\alpha}(\omega) = -i(\omega - n_{\alpha}\omega_e) \frac{C_q^{\alpha} + i\hat{T}_q^{\alpha}(\omega)}{(\omega - n_{\alpha}\omega_e) + C_q^{\alpha} + i\hat{T}_q^{\alpha}(\omega)} , \tag{A9}$$

with

$$C_q^{\alpha} = \langle [\mathcal{H}_{SS}, S_q^{\alpha}] S_q^{\alpha\dagger} \rangle / \langle |S_q^{\alpha}|^2 \rangle$$

and

$$\hat{T}_q^{\alpha}(\omega) = \langle\langle [\mathcal{H}_{SS}, S_q^{\alpha}] | [S_q^{\alpha\dagger}, \mathcal{H}_{SS}] \rangle\rangle_{\omega} / \langle |S_q^{\alpha}|^2 \rangle .$$

The function $\hat{T}_q^{\alpha}(\omega)$ is nothing but the Laplace transform of the Torque correlation function

$$T_q^{\alpha}(t) = \langle e^{i\mathcal{H}t} [\mathcal{H}_{SS}, S_q^{\alpha}] e^{-i\mathcal{H}t} [S_q^{\alpha\dagger}, \mathcal{H}_{SS}] \rangle / \langle |S_q^{\alpha}|^2 \rangle . \tag{A10}$$

As a matter of fact, if we ignore the first term in (A1) which corresponds to the Zeeman Hamiltonian, $T_q^{\alpha}(t)$ is readily seen to be exactly

$$T_q^{\alpha}(t) = -\left\langle \left(\frac{d}{dt} S_q^{\alpha}\right)_t \left(\frac{d}{dt} S_q^{\alpha}\right)_{t=0}^{\dagger} \right\rangle \Big/ \langle |S_q^{\alpha}|^2 \rangle .$$

Therefore, Eq. (A5) gives $\hat{f}_q^{\alpha}(\omega)$ this general form:

$$\hat{f}_q^{\alpha}(\omega) = [i(\omega - n_{\alpha}\omega_e) + \hat{M}_q^{\alpha}(\omega)]^{-1} ,$$

where the memory spectrum $\hat{M}_q^{\alpha}(\omega)$, given by Eq. (A9) is expressed in terms of the torque correlation function (A10).

---

*Present address: Faculty of Education, Physics Department, University of Khartoum, Khartoum, Sudan.

[1] E. H. Lieb and D. C. Mattis, *Mathematical Physics in One Dimension* (Academic, New York, 1966).

[2] For a general review of static properties see L. J. De Jongh and A. R. Miedema, Adv. Phys. 23, 1 (1974); for the dynamic properties see D. Hone and P. M. Richards, Ann. Rev. Mat. Sci. 4, 337 (1974).

[3] N. Bloembergen, Physica 15, 386 (1949).

[4] L. van Hove, Phys. Rev. 95, 1374 (1954).

[5] F. Carboni and P. M. Richards, Phys. Rev. 177, 889 (1969).

[6] N. A. Lurie, D. L. Huber, and M. Blume, Phys. Rev. B 9, 2171 (1974).

[7] R. A. Tahir-Kheli and D. G. McFadden, Phys. Rev. 182, 604 (1969).

[8]F. B. McLean and M. Blume, Phys. Rev. B 7, 1149 (1973).
[9]Z. G. Soos, J. Chem. Phys. 44, 1729 (1966).
[10]R. N. Rogers, F. Carboni, and P. M. Richards, Phys. Rev. Lett. 19, 1016 (1967).
[11]R. E. Dietz, F. R. Merritt, R. Dingle, D. Hone, B. G. Silbernagel, and P. M. Richards, Phys. Rev. Lett. 26, 1186 (1971); R. R. Bartkowski and B. Morosin, Phys. Rev. B 6, 4209 (1972).
[12]T. Moriya, Prog. Theor. Phys. 16, 23 (1956).
[13]S. M. Myers and A. Narath, Phys. Rev. Lett. 27, 641 (1971).
[14]F. Borsa and M. Mali, Phys. Rev. B 9, 2215 (1974); and D. Hone, C. Scherer, and F. Borsa, *ibid.* 9, 965 (1974).
[15]M. Ahmed-Bakheit, Y. Barjhoux, F. Ferrieu, M. Nechtschein, and J-P. Boucher, Solid State Commun. 15, 25 (1974).
[16]J-P. Boucher, F. Ferrieu, and M. Nechtschein, in *Magnetic Resonance and Related Phenomena*, edited by V. Hovi (North-Holland, Amsterdam, 1974), p. 369.
[17]M. J. Hennessy, C. D. McElwee, and P. M. Richards, Phys. Rev. B 7, 930 (1973); see also the more recent works of Z. G. Soos, T. Z. Huang, J. S. Valentine, and R. C. Hughes, *ibid.* 8, 993 (1973); and T. Z. Huang and Z. G. Soos, *ibid.* 9, 4981 (1974).
[18]J-P. Boucher, F. Ferrieu, and M. Nechtschein Phys. Rev. B 9, 3871 (1974).
[19]D. Hone and K. G. Petzinger, Phys. Rev. B 6, 245 (1972).
[20]M. Ahmed-Bakheit, thesis (Grenoble, 1974) (unpublished).
[21]B. Morosin and E. J. Graeber, Acta Crystallogr. 23, 766 (1967).
[22]R. Dingle, M.E. Lines, and S. L. Holt, Phys. Rev. 187, 643 (1969).
[23]B. Vis, C. K. Chan, H. Weinstock, and R. E. Dietz, Solid State Commun. 15, 1765 (1974).
[24]M. T. Hutchings, G. Shirane, R. J. Birgeneau, and S. L. Holt, Phys. Rev. B 5, 1999 (1972).
[25]Y. H. Tchao and S. Clement, J. Phys. (Paris) 35, 861 (1974).
[26]C. Dupas and J. P. Renard, Phys. Lett. A 43, 119 (1973).
[27]The theoretical expression for $T_{1\rho}$ in a paramagnetic crystal can be deduced from the general theory reported by A. Abragam, *The Principles of Nuclear Magnetism* (Clarendon, Oxford, 1961). A theoretical investigation based on a thermodynamical formalism has been recently presented by F. D. Devreux, J-P. Boucher, and M. Nechtschein J. Phys. (Paris) 35, 271 (1974); and erratum (to be published).
[28]P. M. Richards, Phys. Rev. B 10, 805 (1974); J. E. Gulley, D. Hone, D. J. Scalapino, and B. G. Silbernagel, *ibid.* 1, 1020 (1970).
[29]G. F. Reiter and J-P. Boucher, Phys. Rev. B 11, 1823 (1975).
[30]R. Kubo and K. Tomita, J. Phys. Soc. Jpn. 9, 888 (1954).
[31]H. Mori and K. Kawasaki, Prog. Theor. Phys. 27, 529 (1962).
[32]M. Blume and J. Hubbard, Phys. Rev. B 1, 3815 (1970).
[33]P. Resibois and M. De Leener, Phys. Rev. 178, 819 (1969).
[34]J. M. Winter, Ann. Phys. (Paris) 6, 167 (1971).
[35]H. Mori, Prog. Theor. Phys. 33, 423 (1965).
[36]G. F. Reiter, Phys. Rev. B 7, 3325 (1973).
[37]K. Nagata and Y. Tazuke, J. Phys. Soc. Jpn. 32, 337 (1972).
[38]J.-P. Boucher (unpublished).
[39]The sixth moment has recently been calculated exactly by M. Plaindoux, Phys. Lett. A 49, 1 (1974).
[40]One should note that a recent study on another 1*d* Heisenberg system of spin $S=\frac{5}{2}$ ($CsMnCl_2 \cdot 2H_2O$) has given the same result : $D/\omega_x \simeq 2.2$. F. Ferrieu, (private communication).